
Università Cà Foscari Venezia

**Ph.D. Program in Science and technology of bio and nanomaterials**

**XXXIV Cycle**

**Academic Year 2021-2022**

# New drug delivery strategies for antibiofouling

**Supervisor**

Prof. Pietro Riello

**Co-supervisor**

Dr. Andrea Castellin

Prof. Patrizio Raffa

**Ph.D. Candidate**

Mirena Sakaj

*“One never notices what has been done;*
*one can only see what remains to be done.”*

*Marie Curie*

# Acknowledgements

Questo lavoro di tesi di Dottorato è stato tanto desiderato e molto impegnativo, perché risultato di un percorso in cui mi sono rimessa in gioco sia personalmente che professionalmente. Questo percorso mi ha condotta a studiare le infezioni batteriche e come trattarle con metodi innovativi.

Ringrazio sinceramente e con tutto il cuore il mio Tutor, Prof. Pietro Riello, per avermi guidata nel mio percorso di ricerca con preziosi consigli non solo di ricerca ma anche di vita ed insegnato a non mollare mai, condividendo con me i momenti difficili cercando sempre di rallegrarmi.

Ringrazio tutti i colleghi e amici dell'ETA per avermi accolta e supportata in tutto il mio percorso di Dottorato, specialmente Prof. Benedetti, Tiziano, Martina, e Davide ai quali va un ringraziamento speciale e pieno di affetto. Eleonora, Vincenzo e Lorenzo per essere stati dei veri amici e continuano ad esserlo. Prof. Cattaruzza per i nostri piacevoli momenti parlando di libri, musica, giovani e vita.

Un ringraziamento speciale va al Prof. Patrizio Raffa, per avermi accolta nel suo gruppo di ricerca a Groningen, grazie al quale ho potuto studiare i polimeri come drug delivery. Qui ho avuto l'occasione di conoscere Nicola e Mattia che sono stati di grande supporto scientifico e soprattutto amici durante il duro e lungo lockdown in Olanda.

A Francesca Guidi per essere una persona di eccezionale professionalità e pazienza immensa, una persona che porterò sempre nel cuore.

Ringrazio Prof. Alessandro Angelini per il suo supporto scientifico durante i tre anni del mio dottorato insieme al suo dottorando Stefano Pluda.

Un grande saluto va a tutto il campus scientifico per il sostegno e l'apertura riguardo agli esperimenti e strumenti utilizzati in diversi laboratori.

Infine, ringrazio la mia famiglia che crede sempre in me e il mio fidanzato Alessandro per il suo prezioso supporto e le sue infinite attenzioni.

*Mirena Sakaj*

# Table of content

# Figures and Tables

# Abstract

The large current interest in nanomedicine, there has been a rapid progress during the last years in the understanding and the opportunities offered by nanomaterials in diagnosis, drug delivery, biosensors, as well as combination of those as in theragnostic. In the present thesis, focus is placed on drug delivery aspects of inorganic and organic nanoparticles, notably as nanocarriers for peptides against bacterial and biofilm infection.

Bacterial infections and biofilm are sever complication due to the variety of bacteria causing them, their resistance against conventional antibiotics, formation of biofilm and the difficulty to eradicate it. Antimicrobial peptides are naturally occurring peptides and promising candidates for treatment of sever bacterial infections. This thesis aimed to study the effect of short antimicrobial peptides such as temporin B and BmKn2 and analyze them for antimicrobial effect, efficacy on biofilm and their ability to interact with drug delivery systems without losing their activity.

Mesoporous silica nanoparticles were selected as inorganic drug deliver for AMPs, analyzed, tested solo and loaded with the peptides against infections, their capability to protect the peptides from enzyme degradation, together with the ability to reduce antimicrobial peptides toxicity against human cells.

Daptomycin is a lipopeptide antibiotic produced by soil bacterium *Streptomyces roseosporus* and is clinically used to treat sever gram-positive bacterial infections. Daptomycin was used as an antibiotic to evaluate the drug delivery capacity of mesoporous zirconia nanoparticles and the amphiphilic polymer PAA-*b*-PBA. These nanocarriers used for daptomycin delivery present specific pH for the loading

and release, which can be used as targets to infection sites render some benefits over conventional formulation, including stability, permeability, bioavailability and prolonged antibiotic half-life and minimal adverse effects. These nanoparticles are designed to respond to changes in environment of pH to trigger the release of antibiotics.

# Chapter 1

# 1. Introduction

## 1.1. Drug delivery systems

During the last several decades intense effort has been made to develop nanocarriers based on micelles[1], liposomes[2], amphiphilic block copolymers[3], hydrogels as well as inorganic nanoparticles such as mesoporous silica nanoparticles[4], mesoporous zirconia nanoparticles[5] and others. Such systems are in their relative infancy from an industrial development perspective, however, high demands and increasing difficulties to reach efficacy and safety levels required for the introduction of new drugs, including sparingly soluble drugs and bio-macromolecular drugs[6]. For the latter the delivery systems may provide a range of advantages, including conformational stabilization and retained biological activity, protection from chemical and enzymatic degradation, increased bioavailability, control released of drug rate, reduction of toxicity, immunity and other biological effects[7]. The advantage of multifunctional nanoparticle drug delivery systems includes also features as their capacity to improve drug solubility, enhance drug accumulation in the targeting sites and reduce the not desired effects toxicity to a large extend. The term “drug delivery system” can be described as a drug formulation, e.g., tablet, capsule, ointment, and solutions[8]. The term “controlled release drug delivery system” or “controlled drug delivery system” means that a formulation has a built-in technology to control the drug release kinetics over time. The controlled release drug delivery systems are distinguished from conventional formulations that release

most or all loaded drug(s) immediately without any control. Thus, conventional formulations are usually called "immediate release"[9]. The term "controlled release" had an additional meaning of maintaining relatively constant drug concentration once administrated, over time. However, maintaining a constant drug concentration has always been a difficult challenge, especially for oral controlled release formulations[10]. Now days the evolution of drug delivery technology can be described in different ways and began in 1952 as the modern drug delivery technology. Figure 1, describes the developments in drug delivery systems that have shaped the history of controlled drug delivery systems.

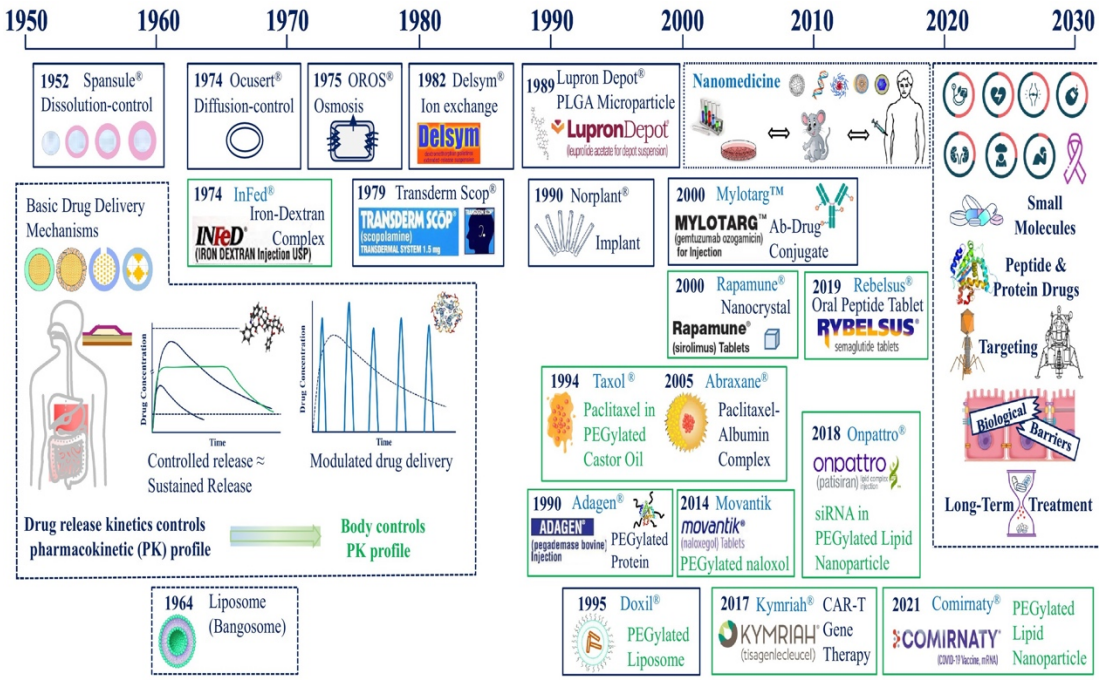


*Fig 1. Historical evolution of drug delivery systems approved from FDA, from the first product developed Spansule® to the lipid nanoparticles formulations for COVID-19 vaccine delivery* [11].

While drug delivery technologies improve constantly, the ultimate measure of the success of a formulation is demonstrated safety and efficacy through the approval by the EMA in Europe and FDA for example in USA, and enabling patients to benefit from the new technologies[12].

Controlled drug delivery systems began with the introduction of Spansule® a 12-hr release technology. The Spansule technology is based in controlling the dissolution of the drug core by a coating barrier that limits the gastrointestinal fluids, thus controlling the dissolution mechanism. A formulation providing a longer duration of release has an equal effect as the immediate release formulation (conventional formulations), as long as the drug delivery systems maintains the concentration of the drug below the maximum safe concentration ($C_{max}$) and above the minimum effective concentration ($C_{min}$). The ration between $C_{max}/C_{min}$ is known as the therapeutic index. Furthermore, the drug delivery systems can minimize the peaks of drugs in the blood, minimizing the side effects and periods of non-efficacy[13].

The United States introduced in the year 2000 the initiative called the "National nanotechnology Initiative", its application to the drug discovery, development and delivery field has been known as Nanomedicine[11]. Still, the outcome has been less than anticipated, registering a small number of new formulations approved. Most of them, especially tumor-targeting of nanomedicine has yet to be achieved, has as primary effect the reduction of side effects of the drugs rather than enhancing the efficacy of the drugs. Nevertheless, by being "nano in size" nanoformulations can improve drug solubility, increasing the dissolutions kinetics of poorly soluble drugs fast enough to release the drug molecules as the dissolved drugs are adsorbed by

the body. Another important improvement by nanomedicine is the research done on the manipulation of lipid nanoparticles to escape from endosomes more efficiently[13]. By realizing that one, the nanoparticles are entrapped by the endosomes, limiting the access to other subcellular components of the cells. Although the process in developing tumor-targeted drug delivery systems by nanomedicine has been slow, such technology has been an ultrafast source of the development of vaccine carries. The lipid molecular and assembled structures have been the key developing COVID-19 mRNA-based vaccines via lipid nanoparticles[14,15].

## 1.2. Nanoparticles and Nanomedicine

Nanoparticles have unique biological properties given their small size (diameter within 1–100 nm) and large surface area to volume ratio, which allows them to bind, absorb agents, such as drugs, DNA, RNA, and proteins, along with imaging agents with high efficiency. Nanocarriers can be classified into two major types designed for targeted or non-targeted drug delivery: vehicles that use organic molecules as a major building block material and those that use inorganic elements. Quantum dots, carbon nanotubes, layered double hydroxides, mesoporous silica and magnetic nanoparticles are used in various ways (Figure 2). NPs have already been proven to be powerful imaging probes, especially for long-term, multiplexed and quantitative imaging and diagnostic[16].

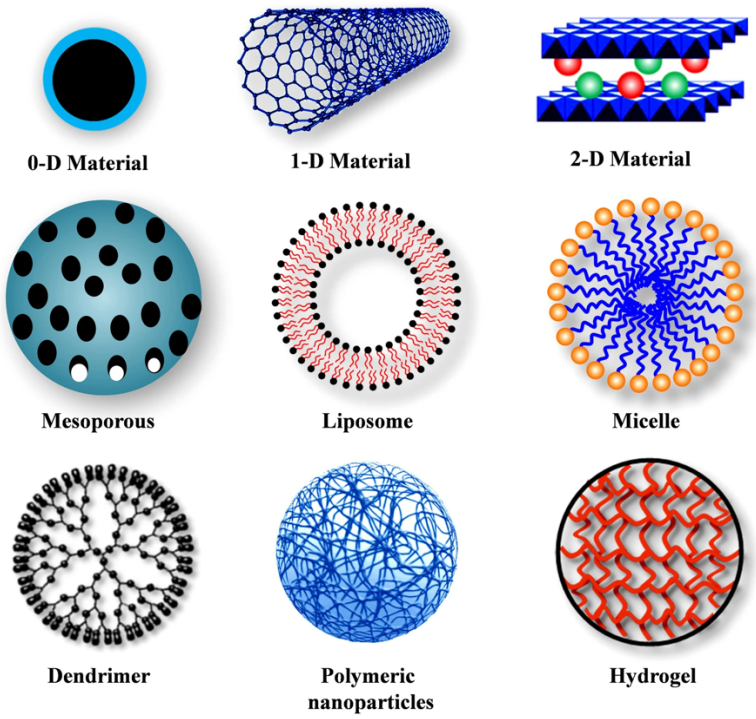


*Fig 2. Types of nanocarriers used in nanomedicine as controlled drug delivery vehicles*[17].

### 1.2.1. Zero dimensional nanoparticles

Zero dimensional (0-D) fluorescent nanoparticles, such as quantum dots (QDs) within the size of 1–10 nm. Zero dimensional nanoparticles have emerged as one of the most promising nanoparticles for targeted and traceable drug delivery systems, real-time monitoring of intracellular processes and in vivo molecular imaging due to their unique physicochemical properties, such as uniform size, large surface-to-volume ratio, biocompatibility, highly tunable photoluminescence property, improved signal brightness, resistance against photo bleaching and multi-color fluorescence imaging and detection[18].

### 1.2.2. Two dimensional nanoparticles

Among the inorganic nanocarriers, two-dimensional (2D) layered double hydroxides (LDHs), also known as hydrotalcite-like compounds, have attracted a great interest for their potential as delivery carriers, mainly because of their biocompatibility, anion exchange capability, high drug loading efficacy, full protection for loaded drugs, pH-responsive drug release, ease of preparation, low cost, easy, and efficient penetration into the cell membrane and considerable drug delivery. Biodegradation in the cellular cytoplasm (pH between 4 and 6), and good endosomal escape; moreover, the drug release rate can be tuned by changing the interlayer anion[1819].

### 1.2.3. Mesoporous nanoparticles

Mesoporous silica nanoparticles (MSNs) are extensively used as drug delivery vehicles due to their unique properties, such as their large specific surface area and pore volume, controllable particle size, ease of functionalizing good biocompatibility and ability to provide a physical casing to protect and house drugs from degeneration or denaturation. MSNs with tunable pore sizes offer great potential for controlling drug loading percentages and release kinetics and can deliver. Another advantage of MSNs is their ability to deliver membrane impermeable hydrophobic drugs, thereby serving as a universal transmembrane carrier for intracellular drug delivery and imaging applications. They also have emerged as promising candidates for both passive and active targeted delivery systems and can accumulate in tumor tissues via the enhanced permeation and

retention (EPR) effect[20]. Furthermore, specific drug delivery can be achieved via active targeting by the functionalizing of MSNs with targeting ligands. Antibodies, peptides, and magnetic nanoparticles can also be decorated onto MSNs, thereby acting as a homing device. In the targeting process, particle size and surface modification of MSNs critically influence particle cellular uptake, pharmacokinetics, and biodistribution profiles[21].

Recently introduced Mesoporous Zirconia Nanoparticles (MZNs) have received much lower attention compared to the above mentioned nanoparticles. Zirconia is a well-known non-toxic biocompatible material exploited for its properties as bulk, in particular in orthopedics and dentistry, just to name two of the most relevant applications. Their toxicological profile is strongly dependent from their dimensions. Recent publications investigated $ZrO_2$ NPs of <100 nm diameter observing toxicity on different Cells and embryonic development of zebrafish, at concentrations of >31 μg/ml and 0,5–1 μg/ml, respectively. MZNs could show important advantages for *in vivo* biomedical applications and for drug loading processes. Recently was reported about the controlled synthesis of new MZNs and demonstrated their biocompatibility and cell permeability and degradability, making them an ideal candidate for theranostic applications[22].

### 1.2.4. Organic nanocarriers

Organic nanoparticles as polymeric nanoparticles are solid, biocompatible, colloidal and often biodegradable systems with nanoscale dimensions[23]. Polymeric nanoparticles are one of the simplest forms of soft materials for nanomedicine

applications due to their facile synthesis and easy structural modification to allow desired properties to be built into the nanoparticle, such as surface modifications to improve drug loading efficacy, biodistribution, pharmacokinetic control and therapeutic efficacy[24]. Polymeric nanoparticles can be made from synthetic polymers, or from natural polymers. Drugs can easily be encapsulated either through dispersion in the polymer matrix or conjugation/attachment to polymer molecules for their controlled delivery through surface or bulk erosion, diffusion through the polymer matrix, swelling followed by diffusion, or as a response to local stimuli[25]. Synthetic polymers have the advantage of sustained release over a period of days to several weeks compared to the relatively shorter duration of drug release of natural polymers; their other benefits include the use of organic solvents and the requirement of typical conditions during encapsulation[26]. Polymeric nanoparticles have therefore been widely investigated as drug delivery systems over the last few decades, including the clinical study of FDA-approved biodegradable polymeric nanoparticles. Doxorubicin has been conjugated with dextran and subsequently encapsulated in a hydrogel using a reverse microemulsion technique reduce its cytotoxic effects and improve its therapeutic efficacy in the treatment of solid tumors. However, by carefully manipulating the drug-to-polymer ratio, molecular weight, and nature of polymer, the extent and level of drug release from nanoparticles can be fine-tuned for effective cancer treatment[26].

Liposomes are small, spherical, self-closed structures with at least one concentric lipid bilayer and an encapsulated aqueous phase in the center. They have been widely used as drug delivery vehicles since their discovery in 1965 due to their

biocompatible and biodegradable nature and their unique ability to encapsulate hydrophilic agents (hydrophilic drugs, DNA, RNA, etc.) in their inner aqueous core and hydrophobic drugs within the lamellae, which makes them versatile therapeutic carriers[27]. Micelles as a drug carrier: Micelles are spherical or globular colloidal nanoscale systems formed by self-assembly of amphiphilic block copolymers in an aqueous solution, resulting in a hydrophobic core and a hydrophilic shell. They belong to a group of amphiphilic colloids that can be formed spontaneously under certain concentrations (critical micelle concentration; CMC) and temperatures[28]. The hydrophobic core serves as a reservoir for hydrophobic drugs, whereas the hydrophilic shell stabilizes the hydrophobic core and renders both polymer and hydrophobic drugs water soluble, making the particle an appropriate candidate for i.v. administration. The drugs are incorporated into a polymeric micelle through physical, chemical, or electrostatic interactions. Multifunctional star-shaped polymeric micelles, based on four-arm disulfide linked poly(ε-caprolactone)-poly(ethylene glycol) amphiphilic copolymers coupled with folate ligands,exhibit high stability and sustained release, whereas prompt release can occur in an acidic environment[29]. Amphiphilic block copolymers (ABP) have received great attention over the past decades due to their ability to self-assemble into stable micelles especially in water. Most importantly, when the water solubility of at least one block is dependent on external parameters such as temperature or pH, they can exhibit stimuli responsive behavior. pH and temperature sensitive copolymers are of pharmaceutical interest to develop controlled release (CR) formulation of certain drugs for their effective targeting to the site of action. The polymeric systems as

drug delivery are used to develop formulations to achieve the maximum concentration to the target site minimizing the side effects. ABP in aqueous media possess clearly separate core-corona structure with size ranges from 1- to 100nm[30,31]. The nano size make them attractive for drug delivery and their high loading capacity together with maintaining their high stability in aqueous environment. Driving force of for their multi-molecular assembly of amphiphilic block copolymers in aqueous media is attributed to their strict differences in water-solubility between individual hydrophobic and hydrophilic blocks. Therefore, the specific molecular design of amphiphilic block copolymers including hydrophobicity/hydrophilicity block length and their ratio is one of the key issues for optimizing their micellar sizes, nanostructures, and longevities in the bloodstream[32].

On the other hand, corona-forming hydrophilic polymer is well known to play a crucial role in reducing the uptake of the micelles from the reticuloendothelial system (RES) and stabilizing the drug loaded micelles in the bloodstream.

Therefore, the biological and pharmaceutical application of ABP is quite attractive in the field of drug delivery and biomaterials applications, a suitable synthesis for controlled molecular weight and distribution is crucial. Among the existing synthesis by radical polymerization techniques, a specific method, reversible addition-fragmentation chain transfer radical (RAFT) polymerization allows us to synthesize well defined polymers using a wide range of monomers under various experimental conditions[33].

## 1.3. pH-responsive carriers

The development of nanotechnology and nanomedicine, nanoparticles show great potential in the treatment of various diseases, including cancer, cardiovascular disease, bacterial, and so forth. Nanoparticles applied to bacterial infections can improve the drug bioavailability, increase the interaction with bacterial cells, inhibit biofilm formation, reduce side effects, and so on. Various antibacterial nanoplatforms are therefore developed to improve the therapeutic performance of bactericidal agents[34]. Although antibacterial nanoplatforms achieved big success, there are still many challenges in the design of the nanoparticles, including targeted accumulation in the infected site, premature drug leakage, slow and incomplete drug release, and so on. To overcome these challenges faced in conventional antibacterial nanoparticles, stimuli-responsive nanoplatforms were extensively investigated to maximize the therapeutic efficacy of bactericidal agents. On one hand, bactericidal agents can be effectively released after specific stimulation, which is a critical step in exerting their actions. On the other hand, the physicochemical properties of the nanoparticles (surface charge, size, etc) can be changed after stimulation, which might be beneficial in enhancing the accumulation and retention in infected tissues, improving the interaction with bacterial cells, enhancing the internalization of bacteria, and increasing the penetration into the biofilms[35].

Stimuli-responsive nanocarriers are specialized nano-sized active delivery vehicles that evolve with an external signal and are equipped with “load-and-release” modalities within their constituting units. The central operating principle of these

drug delivers lies in specific cellular/extracellular stimulus of chemical, biochemical, or physical which can modify the structural composition/conformation of the nanocarriers, thereby promoting release of the active species to specific biological environment[36] (Figure 3).

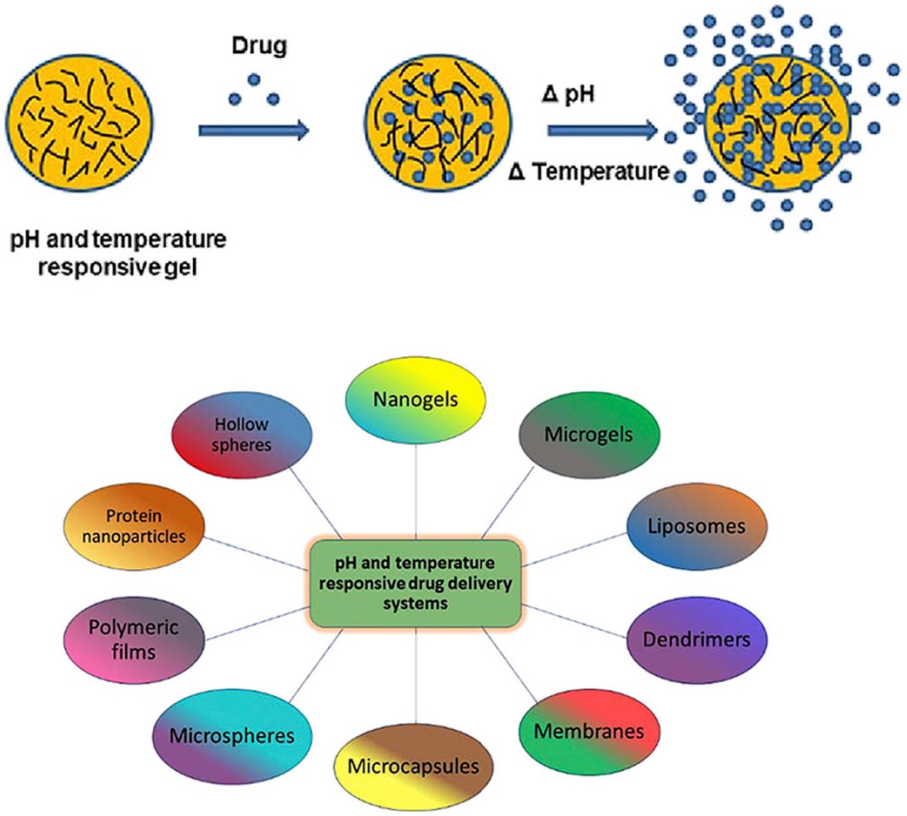


*Fig 3. Stimuli responsive drug delivery systems, such as pH and temperature.*

The general concept of triggered release can be divided mainly into two major modes according to the nature of the interaction between the bioactive molecule and the nanocarriers. In the complexation approach, where the bioactive agent is entrapped within the nanocarrier, the release can be triggered by structural change within the drug deliver (i.e. pH change, carrier degradation, cleavage of shell,

charging of functional groups), while in the nanocarrier-conjugate approach; the mechanism of release involves the splitting of the linker between the carrier and the bioactive agent. The external stimuli which bring about these changes are numerous and cross related[37].

It is known that the infected tissues, bacteria, and biofilms have specific microenvironment, which is different from the normal tissues, due to the immune response and anaerobic glycolysis, the bacterial infections can result in an acidic microenvironment. The specifics of the microenvironment can be used to endogenously trigger specific properties of the nanoparticles, such as drug release, charge reversal, and size change. In theory, the stimuli-responsive behavior of the nanoparticles can only be triggered upon arriving at the infected site, which is very advantageous in improving the drug bioavailability. It is very important that the pH of the microenvironment of the infected site can be served as an endogenous trigger to design pH-responsive nanoplatforms for enhanced antibacterial therapy[38].

## 1.4. Bacterial resistance and biofilm

Antimicrobial resistance (AMR) is recognized as one of the major Global Health challenges of the 21$^{st}$ century by all major regulatory, economic and political bodies. All accept the scientific view that antimicrobial resistance is not simply bounded to the healthcare facilities since most ecosystems contribute to the emergence, acquisition and spread of AMR. As the development of new antibiotics is declining while the resistance is rising, we need to satisfy four goals at one: make antibiotic discovery reasonable; generate antibiotics that address unmet clinical

need; limit unnecessary use of antibiotics; and ensure global access to effective treatment[39].

Antibiotic resistance increases when bacteria adhere to implanted medical devices or damaged tissue and can become the cause of persistent infections. These bacteria encase themselves in a hydrated matrix of polysaccharide and protein, forming slimy layer known as biofilm. When comparing bacteria and bacteria in biofilm, familiar resistance mechanism of antibiotics, such as efflux pumps, modifying enzymes and target mutations, do not seem to be responsible for the protection of bacteria in biofilm[40] (Figure 4).

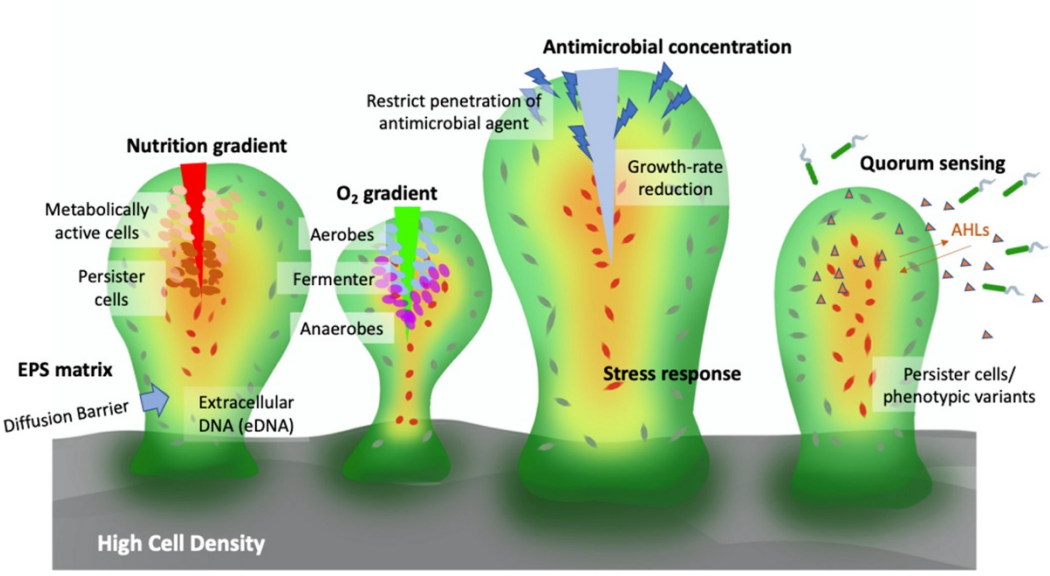


*Fig 4. Schematic representation of biofilm resistance to antimicrobials*[41]

Biofilms are composed of bacteria that irreversibly adhere to the surface of living or non-living organisms and are surrounded by a secreted matrix of extracellular polysaccharide, protein, and DNA. Once the special structure forms, the bacteria express completely different genes from planktonic bacteria, with significant

differences in morphology, physical and chemical properties, and antibiotic susceptibility[42]. At the same time, it is beneficial for bacteria to survive on nutritionally limited abiotic surfaces and stressful environmental conditions. Bacterial biofilms cause at least 65% of human infections, particularly implantable device-related infections and chronic disease infections. Therefore, there is an urgent need for drugs that effectively treat biofilm-associated infections. At present, it has been reported that some natural product extracts and compounds can treat bacterial biofilms[43]. Ursolic acid can inhibit the formation of biofilms, while resveratrol combined with vancomycin can inhibit pre-formed mature biofilms. Silver nanoparticles do not affect the growth of planktonic *Staphylococcus aureus* but can reduce the production of biofilms at a concentration of 50 μg/ml. However, in many cases, these anti-biofilm active ingredients are not sufficient enough to completely inhibit or eliminate bacterial biofilms and lack broad-spectrum anti-biofilm efficacy[44].

## 1.5. Antimicrobial peptides

Antimicrobial peptides (AMPS) are important key components of innate immune system, produced as a first line of defense by all multicellular organisms. AMPs can have a broad activity to directly kill bacteria, yeast, fungi viruses and even cancer cells. Plants and insects deploy AMPs as an antibiotic to protect against pathogenic microbes, and also microbes produce AMPs to defend their environment. In higher eukaryotic organisms, to emphasize their additional immunomodulatory activity can be also referred as "host defense peptides"[44].

AMPs have been recognized since 1939 when antimicrobial substances, named gramicidins, were isolated from *Bacillus brevis*, and were found to exhibit activity both *in vitro* and *in vivo* against a wide range of Gram-positive bacteria. Gramicidins were later shown to treat wound guinea pig skin and were the first AMPs to be commercially available[45].

At the end of 1920s, lysozyme was identified by Alexander Fleming and is considered by some authors the first reported instance of peptide with antimicrobial activity[46]. In 1928, Fleming discovered penicillin and in the 1949s, along with Howard Florey and Ernest Chain, he brought the therapeutic use of penicillin to fruition, which led these three men to share the 1945 Nobel Prize for Medicine. With the advent of penicillin and streptomycin in 1943, began the "Golden Age of antibiotics" which led to a rapid loss of interest in the therapeutic potential of natural host antibiotics such as lysozyme and the importance of this immune defense strategy[47].

In the early 1960s, with the rise of multidrug-resistance microbial pathogenes, and realizing that "Golden Age of antibiotics" has ended an awakened interest in host defense molecules was prompted. It is this point in time that some sources consider to be the true origin of research into AMPs, when it was shown that cationic peptides were responsible for the ability of human neutrophiles to kill bacteria via oxygen independent mechanisms not activity associated with the adaptive immune system. In the late 1970s and 1980s several groups reported a number of AMPs and antimicrobial proteins from leukocytes, including what we now know to be α-defensins from rabbits and humans. In 1981, in what are now generally considered as a landmark study, Boman et al. injected bacteria into the pupae of the silk moth, *Hyalophora cectropia*, and isolated the inducible cationic antimicrobial proteins, P9A and P9B, from the hemolymph of these pupae[48]. These peptides were sequenced, characterized, and renamed as the more familiar "cecropins", thereby constituting the first major α-helical AMPs to be reported.

In the early 1990s, evidence began to accumulate that led to the current view that lysozyme possesses antimicrobial activity involving non-enzymatic mechanism that are similar to AMPs, thereby substantiating the view that it was one of the first of these peptides to be discovered[49].

Since these earlier studies, AMPs have been extensively studies, although most of the current understanding of AMPs has been obtained from studies on those isolates from amphibian skin secretions which is a rich source of these peptides[50].

Nonetheless, it is now well established that the production of the AMPs is a defense strategy used across eukaryotes, evidenced by the list of databases dedicated to

these peptides that have appeared almost every year over the last decades. According to these databases, more than 2000 AMPs have been listed and the number of these peptides is rapidly increasing and classified based on a variety of criteria, most often structure-function relationship, and mechanism of antimicrobial action[51].

## 1.5.1. Mechanism of action of antimicrobial peptides

The unique ability of AMPs to control infections as well as resolve harmful inflammation has generated interest in harnessing the properties of these peptides to develop new therapies for infection diseases.

Over the last three decades there has been a substantial interest in therapeutically harnessing AMPs, with more than 5,000 articles in this area since 2017 alone. Publications examine the potential use in clinic of AMPs, including infections involving multidrug-resistance bacteria, chronic inflammatory diseases, as well as some cancers. Clinical trials of peptide-based therapeutics are primarily intended for the treatment of infections such as respiratory tract, oral and catheter-related infections, and for wound healing. AMPs have multiple targets, such as DNA, RNA, protein synthesis, but the main origin of their antimicrobial effect is lysis of bacterial membrane. The selectivity towards bacterial membrane is central to the therapeutic function of AMPs so the bacterial are efficiently killed but human cells left intact. This selectivity is due to the differences between human and bacterial cell membranes. Human cells, for example, are rich in cholesterol, fungal membranes contain ergosterol, whereas bacterial membrane has no sterol at all.

Furthermore, human cells are zwitterionic, dominated by lipids such as phosphatidylcholine and sphingomyelin, thus being generally uncharged, while bacterial membrane are highly anionic. In addition, the outer membrane of Gram-negative bacteria contain anionic lipoteichoic acid (LTA) and Gram-positive bacteria is rich in highly anionic lipopolysaccharide (LPS). While terms like "pore and ion-channel" are used for AMP-induced membrane defects, there is a growing evidence that very few AMPs forming well defined pores (Figure 5). Instead, these peptides mostly form small, disoriented, and transient defects[52].

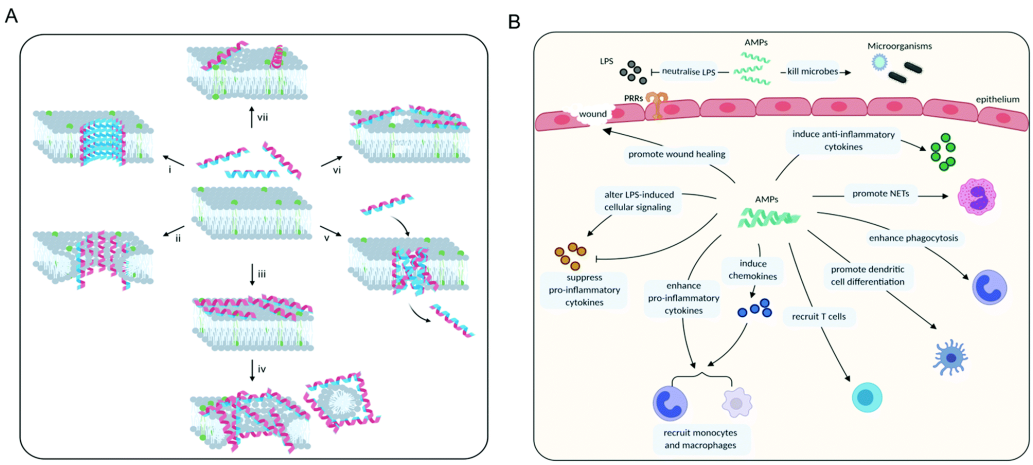


*Fig 5. A) Mode of action of AMPs in disrupting membranes of pathogenes, B) mode of action of AMPs against intracellular targets.*

Due to the anionic nature of bacterial membranes, the net positive charge of AMPs is key for membrane lysis. Formation of amphiphilic conformations, especially α-helical, has been found to contribute to peptide binding, membrane disruption, and bacterial killing[53,54]. Comparable, suppression of amphiphilic helix formation has been correlated to increase AMPs toxicity related to disruption of eukaryotic cell membrane[52].

Hydrophobicity plays a fundamental role in AMPs potency, with the increasing of hydrophobicity peptide activity against bacterial increases, especially at high ionic strength, in the presence of serum, or for low charged pathogens. This parameter has been found to be a fundamental key for antimicrobial effect in a number of quantitative structure-activity-related (SAR) investigations[54–56]. For very hydrophobic peptides, however, peptide binding occurs regardless of membrane composition, resulting in lysis of both bacteria and human cells, with really little or no discrimination. For example, hydrophilic K/L peptides are even more hemolytic than bee venom melittin, thus hydrophobicity can only be used to some extent to boost AMP potency without losing selectivity.

Singh *et al.* demonstrated that while membrane binging of a series of S1 peptidases is largely driven by conformation-dependent amphiphilicity of these peptides, LPS binding depends on peptide net charge, as well as well as hydrophobicity[57].

The primary mode-of-action behind antimicrobial effect of AMPs is the disruption of bacterial membranes. There is a good correlation between bacteria killing, bacteria lysis, lysis of "bacterial mimicking" liposome membranes, peptide adsorption to such lipid membranes. Numerous parameters are of importance for AMP-membrane interaction including peptide length, charge (distribution), hydrophobicity distribution, and secondary structure[58].

## 1.5.2. Antimicrobial peptides used in this thesis

### 1.5.2.1. Temporin B

Frog skin is one of the richest sources of the AMPs that are synthetized by adrenergically innervated dermal glands and stored within granules that are released onto skin surface by holocrine mechanism in response to alarm or injury. A family of amphibian AMPs, originally isolated from the European red frog *Rana temporaria*, is called temporins. These peptides represent the shortest AMPs found in nature to date with typical length of 10 to 13 amino acids and a conserved sequence. They are amidated at the C terminus and are characterized by a weak cationic charge (net charge ranging from +1 to +3) owing to the presence of only one or two positively charged amino acids, such as lysine or arginine, in their sequence.

Temporins, are attractive templates for the development of antibiotics[59], like other AMPs exert antimicrobial activity against mycetes and bacteria, while their antiviral activity has been reported only against few enveloped or nonenveloped viruses of ectothermic animals and inhibits *in vitro* herpes simplex virus 1 infection[60].

Temporin b has gained increasing attention as novel antimicrobial agents for the treatment of antibiotic-resistant and/or biofilm mediated infection. Temporin B possesses a preferential spectrum of action of action against Gram-positive bacteria. Temporins minimum inhibition concentration (MIC) against Gram-positive bacteria values ranges from 2.5-20μM and weak activity against Gram-negative bacteria such as *Escherichia col*[61]*i*.

By contrast to other temporins like temporin L, temporin B was demonstrated together with temporin A displaying non-hemolytic and non-toxic characteristics to normal human cells, suggesting their potential therapeutic values[62,63].

### 1.5.2.2. BmKn2

The scorpion venom of the hole tail has been used as main Chinese traditional medicine to treat neurological diseases for more than 2000 years. Therefore, it is very interesting that further insights have identified different antimicrobial peptides from the venom gland of *Buthus marternsii* Karsch. BmKn2 is a basic alpha-helical antimicrobial peptide with no sulfide bond derived from *B. martensii* Karsch species. BmKn2 is 13 amino acids long, with two positive net charges and a molecular weight of 1447.8 Da. BmKn2 has strong activity against Gram-positive bacteria and weak activity against Gram-negative bacteria including *Staphylococcus aureus, Bacillus subtilis, Escherichia coli, Pseudomonas aeruginosa and Neisseria gonorrhoeae*[64]. This antimicrobial peptide also exert anti-cancer activity against oral and colon cancer cells[65,66]. Nevertheless, to best of our knowledge, experimental data regarding the antibiofilm activity of this peptide against *S. aureus* and *E. epidermidis* has not yet been reported. The present thesis therefore evaluated antibiofilm activity of BmKn2 peptide against *S. aureus* and *E. epidermidis*.

## 1.6. Daptomycin

Daptomycin is a member of the A21978C group of calcium-dependent, cyclic lipopeptide antibiotics that were originally isolated from the fermentation of Streptomyces roseosporus by researchers at Eli Lily in the early 1980s. Daptomycin showed excellent activity against a variety of Gram-positive organ- isms, but they were inactive against Gram-negatives. Eli Lily began the clinical development of daptomycin in 1985, but later abandoned it when they observed myopathic side effects during Phase II trials[67]. In 1997, Cubist Pharmaceuticals Inc. (recently acquired by Merck & Co.) licensed daptomycin and resumed clinical testing. They found that the myopathic side effects could be minimized by altering the dose regimen. These successful tests resulted in approval for clinical use beginning in 2003. Daptomycin was approved for clinical use in the USA in 2003, and in Europe in 2006, for treating complicated skin and skin-structure infections caused by methicillin-susceptible and -resistant *S. aureus* (MSSA and MRSA), *Streptococcus pyogenes, Streptococcus agalactiae, Streptococcus dysgalactiae subsp. equisimilis*, as well as vancomycin-susceptible *E. faecalis*[68]. Although many cyclic lipopeptide antibiotics have been discovered, daptomycin remains the only member of this class that is approved for clinical use. A notable gap in the clinical action spectrum of daptomycin is *Streptococcus pneumoniae*, the leading cause of community-acquired pneumonia. While *S. pneumoniae* is highly susceptible in *vitro*, this does not translate into sufficient therapeutic activity in *vivo*. The likely cause for this discrepancy is the inhibition of daptomycin by lung surfactant, which binds and sequesters the drug. The inhibition may be related to its content of

phosphatidylglycerol. Efforts have been made to develop daptomycin derivatives that avoid surfactant inhibition[69].

Daptomycin and all other members of the A21978C group of lipopeptides are synthesized by the same modular non-ribosomal synthetase system and contain the same peptide moiety; the only part of the structure that differs between them is the N-terminally attached fatty acyl residue (Figure 6).

The nature of the fatty acyl residue affects both antibacterial activity and toxicity; a decanoyl residue imparts the most favorable combination.

Daptomycin has six amino acid residues with ionizable side chains: four acidic residues and two residues containing primary amino groups. The pKa values of these residues in the absence of Ca2+ have been characterized by potentiometric titration, ultraviolet (UV) spectrophotometry, and NMR spectroscopy[70].

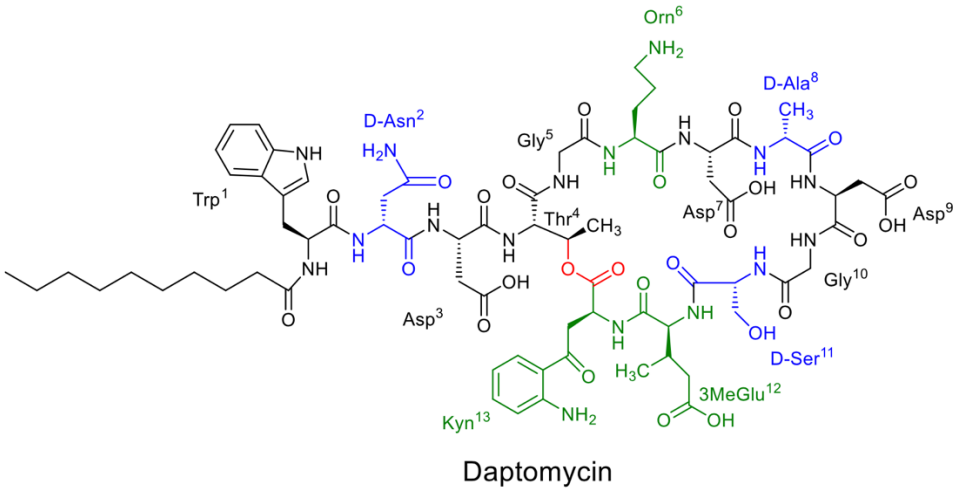


*Fig 6. Daptomycin structure representation.*

NMR studies carried on daptomycin in solution indicate that Ca2+ binds to daptomycin in a cooperative manner and with a 1:1 stoichiometry. Therefore, the

Ca2+- bound form of daptomycin in solution exists as a monoanion. Daptomycin's amphiphilic structure suggests that it may form aggregates in solution. In the absence of calcium and at pH 7.4 or higher, daptomycin aggregation is minimal or absent at millimolar concentrations, whereas under acidic conditions aggregates may form at concentrations as low as 0.12–0.2 mM. This pH- dependent variation can be explained by the ionization state of apo-daptomycin. Between pH 2.5 and 4, apo-daptomycin exists primarily as a neutral or monoanionic species. As the pH increases to 7, deprotonation of Asp(3) and mGlu(12) will cause the dianionic and trianionic forms to dominate[71].

# Chapter 2

# 2. Materials and Methods

## 2.1. Materials

Fmoc-protected amino acids, Rink Amide AM resin support and benzotriazol-1-yloxytripyrrolidinophosphonium hexafluorophosphate) (PyBOP) were purchased from Novabiochem. Trifuoroacetic acid (TFA), Triisopropylsilane (TIS), cetyltrimethylammonium bromide (CTABr), tetraethyl orthosilicate (TEOS), $Na_2HPO_4$, $NaH_2PO_4$, R6G, $K_3PO_4$,$CaCl_2$, $Na_3C_6H_5O_7$, dialysis tubing cellulose membrane, Nutrient broth (NB), NaF, HCl (37%), NaCl, $Zr(OPr)_4$ solution, from Fluka. 1- hexadecylamine from Alfa Aesar. Proteinase K, phosphate-buffer saline (PBS) and Agar were purchased from Sigma Aldrich. Staphylococcus aureus ATCC 25923 and Escherichia coli ATCC25922 strains were obtained from the American Type Culture Collection. Calgary biofilm assay (CBD) was purchased from Innovotech.

## 2.2. Methods

### 2.2.1. Peptide synthesis

Temporin B (LLPIVGNLLKSLL) and BmKn2 (FIGAIARLLSKIF) were synthesized on the MultiPep RSi synthesizer (Intavis) by standard Fmoc solid-phase chemistry on a Rink Amide AM resin (0.01 mmol scale, 100 - 200 mesh

loading 0.52 mmol/g). Coupling step was carried out twice for each amino acid (6 eq, 0.4 M solution in DMF) using PyBOP (5.5 eq, 0.4 M solution in DMF) NMM (9 eq, 4 M solution in DMF) coupling system. Fmoc groups were removed using a 20% (v/v) solution of piperidine in DMF. The final peptides were deprotected and cleaved from the resin using a TFA/TIS/water/ mixture (95/2.5/2.5 v/v) for 3 hours at room temperature under vigorous shacking. The peptide was precipitated with cold diethyl ether (50 ml), centrifuged, resuspended and washed with diethyl ether (20 ml x 2). The peptide was further purified by preparative reversed-phase high performance liquid chromatography (RP-HPLC) C18 column, linear gradient with a mobile phase composed of eluent A (99.9% v/v $H_2O$, 0.1% v/v TFA) and eluent B (99.9% v/v acetonitrile, 0.1% v/v TFA) and a flow rate of 20 mL/min. The purified peptides were freeze-dried and dissolved in $H_2O$ mQ. The purity of the peptides was assessed by analytical RP-HPLC (LC Perkin Elmer). The molecular mass was confirmed by Liquid Chromatography Mass Spectrometry (LC/MS) analysis (Agilent 1260 Infinity).

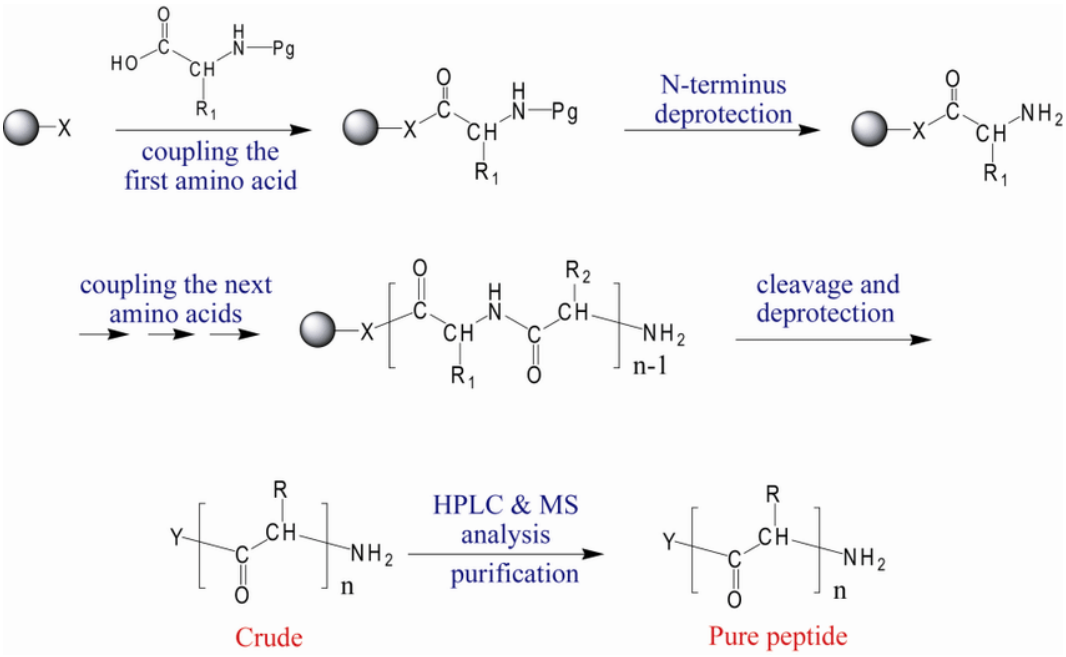


*Fig 7. Schematic representation of solid phase peptide synthesis.*

Due to absence of aromatic residues in the peptides sequence, the concentrations were extrapolated from calibration curves generated using six different concentrations in the range (0.5 mg/ml – 0.015 mg/ml) using RP-HPLC C18 column, at a wavelength of 220 nm, and a linear gradient with a mobile phase composed of eluent A (99.9% v/v $H_2O$, 0.1% v/v TFA) and eluent B (94.9% v/v acetonitrile, 5% v/v H2O and 0.1% v/v TFA) and a flow rate of 1 mL/min. The calibration curves show a good linearity in the analyzed range ($R^2$=0.999).

## 2.2.2. Mesoporous silica nanoparticles synthesis

Mesoporous silica nanoparticles (MSNs) were synthesized as described elsewhere [72]. In a glass flask was dissolved in water (142 ml) and ethanol (48 ml) solution a

quantity of CTABr (5.7 g) and ammonia solution (0.38ml) under stirring at room temperature for 15 min at 500 rpm. After the complete solubilization of the compounds, TEOS (5 ml) was dropped, and the mixture stirred vigorously (500rpm) for 2 h at 30 °C. The final colloidal solution was centrifuged at 30000g and the recovered solid was washed several times with ETOH and $H_2O$ (50% v/v) and dried at 60 °C overnight. To remove the surfactant, the product was calcined at 550 °C, with a rate of 2 °C/min for 5 h. The obtained sample was referred to as MSN.

### 2.2.3. Mesoporous zirconia nanoparticles synthesis

In a flask of 250 ml 0,908g of hexadecylamine were dissolved in 90,26 ml of ethanol under vigorous stirring at room temperature. 0,622 ml of MilliQ water and 0,366 ml of NaF 0,1 M were then added to this solution. In a vial 0,909 ml of the precursor, $Zr(OPr)_4$, was mixed with 1,143 ml of EtOH, under stirring for 15 minutes, until the two phases disappear and the solution became clear and yellow. This second solution was added dropwise into the first solution under stirring and left overnight at room temperature. Nanoparticles formation turns the clear solution into a white and opaque dispersion. Nanoparticles are then collected centrifuging the solution at 12500 g for 20 minutes and washed three times with EtOH. The resulting pellet was dried overnight. The dry powder was weighed and put in a Teflon bomb with 12,5 ml of EtOH and 6,25 ml of MilliQ water per gram of sample. The dispersion was left under stirring for an hour, and then put in an oven at 170°C

for 16 hours for the hydrothermal treatment. After this, the powder was filtered and washed with ethanol and water and left to dry. In order to extract the surfactant, the powder was put in a flask under vacuum (0,05 mbar), in an oil bath on an hotplate at 125°C. Extraction was allowed to proceed overnight and in the end the powder was filtered and washed with EtOH and water.

### 2.2.4. Amphiphilic polymers synthesis

Polyacrylic acid macro-RAFT (PAA-MacroRaft) was synthesized by RAFT. RAFT agent CTPPA (mg), AIBN() and monomer acrylic acid were dissolved in ethanol in round-bottom flask equipped with a magnetic stirrer. The flask was sealed, and the solution was degassed with argon for 45 min. polymerization was conducted for 7hr at 70°C. In predetermined reaction times, a certain amount of sample was collected by a syringe and dissolved in DMSO-$d_6$ to determine the AA conversion by $^1$H-NMR. After complete polymerization, the PAA-macroRAFT was isolated by precipitation in diethyl ether, filtered, dialyzed, and dried under vacuum at 40°C for 24 hours. The PAA-macroRAFT was further freeze-dried to remove traces of solvents and therefore dissolved in DMSO-$d_6$ for $^1$H-NMR analysis. PAA-b-PBA nanoparticles was synthetized starting from PAA-macroRAFT, which was dissolved in dioxane in a round-bottom flask equipped with a magnetic stirrer, AIBN() was added and *n*-BA. The flask was sealed and the mixture was degassed by argon for 45min. The reaction was conducted for 7hr and every predeterminate

reaction times, samples were collected, dissolved in DMSO-$d_6$ for $^1$H-NMR analysis. Size exclusion chromatography was used to determine the conversion of monomers into polymer.

### 2.2.5. Antimicrobial peptides/Daptomycin loading

Temporin B and BmKn2 0.5 mg were incubated with 1 mg of MSNs in phosphate buffer saline at pH 5.5, 7.4 and 10 for 24 h. Unadsorbed peptides were separated from the MSNs by centrifugation at 12 000 rpm for 10 min, washed twice to remove the remained unadsorbed peptides and the concentrations were measured after 24 hours using RP-HPLC C18 column with the procedure described in section 2.2.1.

Daptomycin 1mg was incubated with 2mg of MZNs in phosphate buffer at pH 5, 7,4 (isotonic solution) and 9. Unloaded antibiotic was removed by centrifuging at 12 000 rpm for 10 minutes, washed twice with the same buffer used for the loading and centrifuged again, in order to make sure to remove the non-loaded antibiotic. Daptomycin concentration was measured by UV visible spectrophotometer at 260nm, with a calibration curve at the range of 1000µg/ml – 0.001µg/ml.

### 2.2.6. Antimicrobial peptide release

pH-triggered efficiency release of temporin B and BmKn2 and daptomycin from loaded MSNs/MZNs were assessed at different pH values (5.5, 7.4 and 10). Released peptides/antibiotic were separated from the MSNs/MZNs by centrifugation at 12000 rpm for 10 min. The peptides concentrations were measured at different time points using RP-HPLC C18 with the described procedure and daptomycin using UV visible spectrophotometer.

### 2.2.7. Antibacterial and antibiofilm activity

Antimicrobial activity was determined by standard liquid dilution method in Nutrient Broth (NB) medium. S. aureus ATCC25923 cells were grown overnight at 37 °C in NB and diluted in the same medium for assays. In 96-well sterile microtiter tray, 50 µL of bacteria from overnight culture (adjusted to $1x10^6$cells/ml) was added to the serial dilution of the samples. Positive controls were tested and final concentration PBS as blank, in a total volume of 150 µl of NB. The 96-well microtiter tray was placed at 37 °C for 24 hours and the cells growth assessed by measuring the optical density at 600 nm with a Synergy - Biotek microplate reader. MICs (minimum inhibition concentrations) were determined as the lowest peptide concentration that inhibits 100% of bacteria growth.

Antibiofilm activity was determined using the assay Calgary biofilm assay (CBD), a 96 well plate with pigs built into the lid. Each peg provides a surface for the

formation of biofilm. Bacteria was cultured in NB medium and allowed to form biofilm for 24 hours. Once the biofilms are formed, the lid (with the pegs) is rinsed and placed onto flat-bottom microtitel plates, where they can incubate for other 24 hours at 37°C in the presence of different concentration of antimicrobial peptides. Then the pegs are again rinsed and transferred into an antimicrobial free medium in a biofilm recovery plate. The plate is then sonicated for 30-min in order to transfer the biofilm from the pegs to the fresh medium in the plate. After 10-fold of serial dilution for each concentration (including positive and negative controls) samples of 20µl are transferred into NB-agar plates, incubated for 24 hours at 37°C and the MBEC was determined by colony counting.

Crystal violet biofilm assay. The biofilm assay was conducted in 96-well polystyrene flat-bottomed microplate. Firstly, the *S. aureus ATCC25923* suspension at $1x10^6$cells/ml was prepared and dispended into each well in 96-well plate. The microplate was then incubated for 24 hours to allow the biofilm formation, growth and attach to the wells. To screen for antibiofilm activity, after 24 hours of incubation 37°C the samples were added to the desired concentrations and dilutions in duplicate wells, representing the two technical replicates. As control the bacteria were incubated with the same amount of PBS the samples were suspended. Uninoculated broth wells were also included as blank control. Then the microplate was again incubated for 24 hours at the same conditions. After incubation the wells were washed twice with sterile mQ water, twice with phosphate buffer saline and to remove the not adherent cells bacteria was fixes with 99% methanol for 15 minutes. The methanol was removed, and the cells were

allowed to dry in a laminar flow. The attached biofilm was stained with crystal violet 0.5% for 5 minutes at room temperature. The excess stain was removed by rinsing with water and the crystal violet bound cells were solubilized with 33% acetic acid. The release stain was measured at 570nm using a microplate reader.

### 2.2.8. Proteolytic stability

Peptides loaded in MSNs, as described above at pH 10, were used to investigate the proteolytic protection by incubating the loaded 0.42 mg/ml temporin B in 1 mg/ml of MSNs and 0.45 mg/ml BmKn2 in 1 mg/ml of MSN with proteinase K (10 µg/ml) in PBS at pH 7.4. Mixtures were incubated at 37 °C in a thermo block. After 4, 8 and 16 hours, 100 µl samples were taken, mixed with 100 µl of filtered-sterilized $H_20$ with 0.1% v/v TFA to quench the reaction, centrifuged at 12 000 rpm for 10 min and characterized using RP-HPLC C18 column at a wavelength of 220 nm, and a linear gradient with a mobile phase composed of eluent A (99.9% v/v $H_2O$, 0.1% v/v TFA) and eluent B (94.9% v/v acetonitrile, 5% v/v H2O and 0.1% v/v TFA) and a flow rate of 1 mL/min. (24).

### 2.2.9. Cytotoxicity

Lung fibroblasts (MRC-5) were grown at 37 °C in a controlled atmosphere containing 5% $CO_2$ according to the supplier instructions. A thousand of cancer cells were plated in 96-multiwell culture plates or 5000 cells for MRC-5. The day after seeding, drugs were added with a serial dilution 1:10 to have a final concentration ranging from (1000 µg/mL) to (0.01 µg/mL). Cell viability was measured with Tecan Infinite M1000 PRO (Tecan, Mannedorf, Switzerland) after 96 h with CellTiter-Glo® assay according to the supplier (Promega, Madison, WI, US). $IC_{50}$ values were calculated from nonlinear regression dose–response curves by GraphPad Prism 8 Software. Averages were obtained from triplicates and the errors are standard deviations.

# Chapter 3

# 3. Results and discussion

## 3.1. Antimicrobial peptides as antibacterial agents

Temporin b and Bmkn2 are two antimicrobial peptides from animal origin. These two antimicrobial peptides are short, linear, cationic belonging to the family of $\alpha$ -helical antimicrobial peptides were selected, synthetized, characterized and tested for antibacterial activity.

After the cleavage and precipitation, the peptides were diluted in milli-Q water and purified with HPLC preparative at 220nm followed by analytical measurement with reverse phase high pressure liquid chromatography (RP-HPLC) in which every antimicrobial peptide represent a given retention time as showed in Figure 9. Mass spectrometry confirmed the successful synthesis with MultiPep RSi synthesizer (Intavis). In Figure 8 are shown the mass spectra and in figure 9 the chromatograms of the antimicrobial peptides after the purification. The synthesis was performed several times with same results.

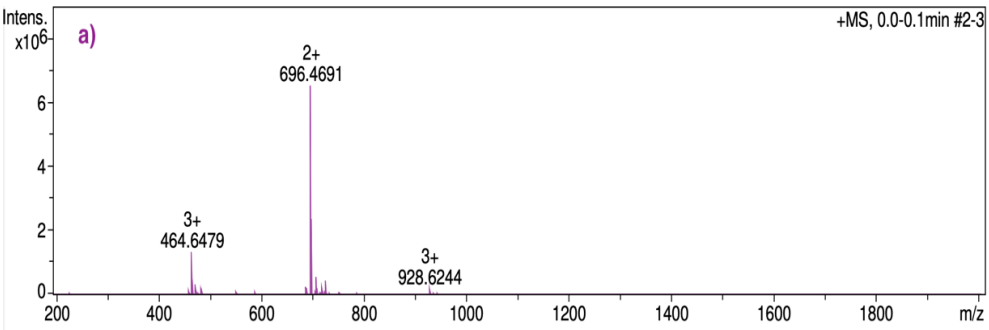

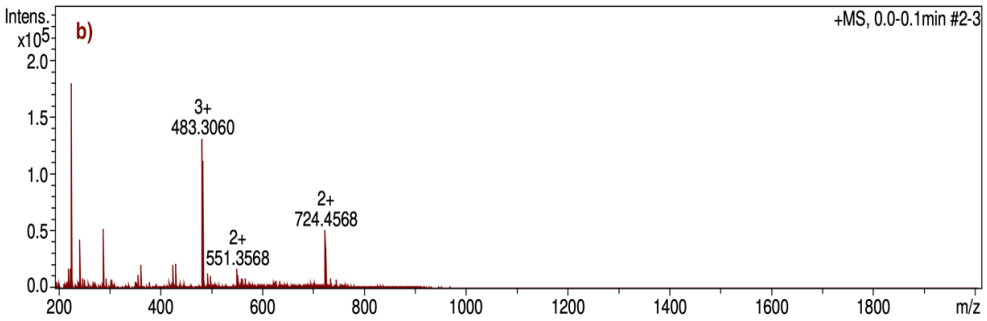


*Fig 8. Full scan ESI⁺ mass spectra's of a) temporin B and b) BmKn2 generated in the positive ion mode with the adding of 0.1% formic acid.*

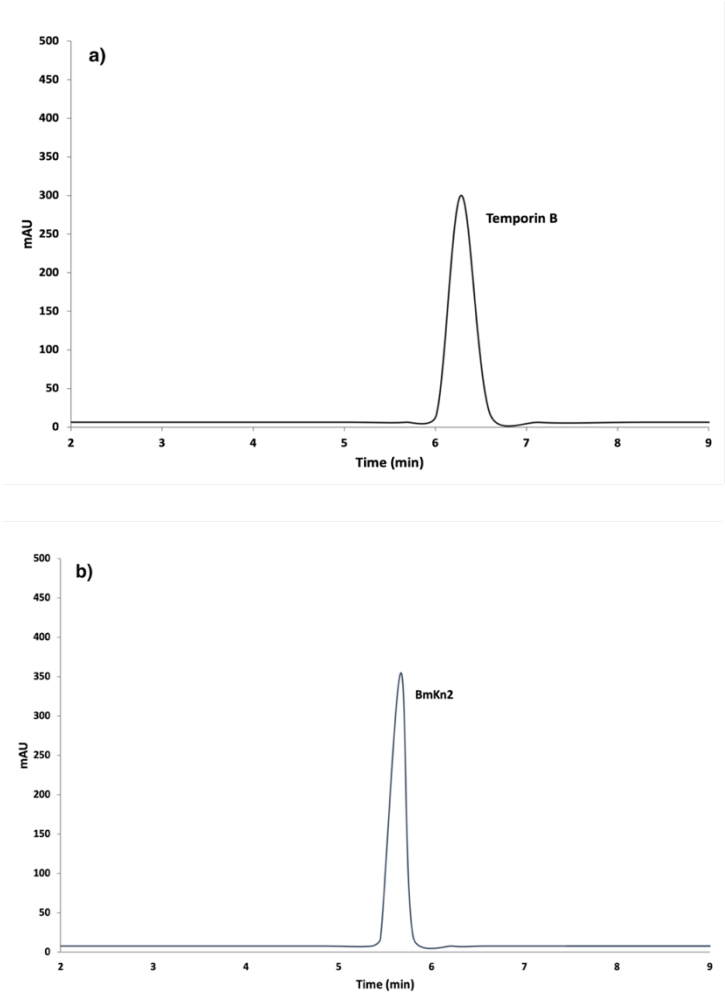


*Fig 9. The HPLC chromatograms of **a)** temporin B and **b)** BmKn2. The HPLC profiles were measured at 220nm in acetonitrile/water with 0.1% of TFA.*

The antibacterial activity screening of different concentration of the antimicrobial peptides was determined for two strains *S. aureus ATCC25923* and *E. coli ATCC25922,* Gram-positive and Gram-negative respectively as the minimum inhibition concentration, summarized in Table 1 set with general information of the two antimicrobial peptides.

**Table 1.** Sequence, origin, characteristics, and MICs of antimicrobial peptides

| **Characteristics** | **Temporin B** | **BmKn2** |
|---|---|---|
| **Origin** | skin frog | scorpion venom |
| **Sequence** | LLPIVGNLLKSLL | FIGAIARLLSKIF |
| **Length** | 13 | 13 |
| **Hydrophobicity** | +4.22 Kcal*mol$^{-1}$ | +5.84 Kcal*mol$^{-1}$ |
| **Charge** | +1 | +2 |
| **Molecular weight** | 1391.9 Da | 1447.9 Da |
| **MIC *E. coli ATCC25922*** | >100µg/ml | >100µg/ml |
| **MIC *S. aureus ATCC25923*** | 12.5µg/ml | 6.25µg/ml |

The highest concentration used was 100µg/ml, which was high enough to determine the MICs for the Gram-positive strain, but with moderate activity and not enough high to determine the MICs for the Gram-negative strain, showing in this case specificity based on the concentration (>20µg/ml) against *S. aureus ATCC25923*. The most active peptide is BmKn2, containing two positive charges which increases its antibacterial activity against Gram-positive and the moderate but still higher activity towards Gram-negative bacteria as shown in Figure 10. The two positive charges are more likely to interact with the negatively charged outer membrane of both strains, as mentioned above.

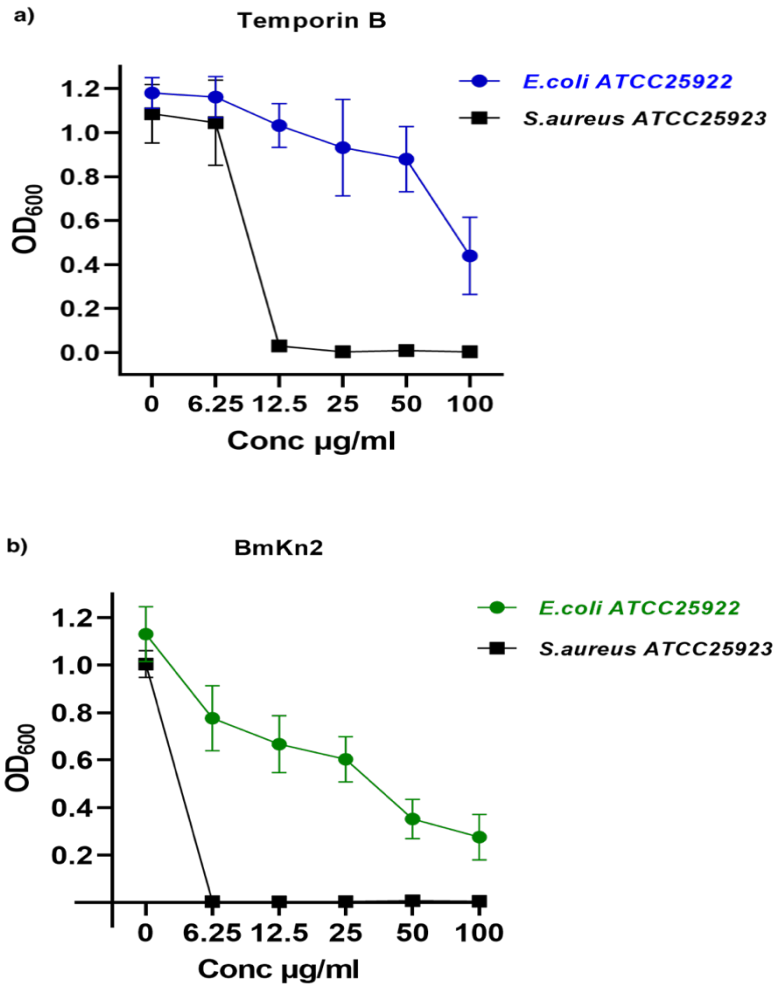


*Fig 10. Antibacterial activity of a) temporin B and b) BmKn2 against S. aureus ATCC25923 and E. coli ATCC25922. Bacteria were incubated in nutrient broth (pH 6.5 - 7) with the peptides and concentrations ranging from 100µg/ml – 6.25µg/ml. Untreated bacteria were used as positive control.*

This comparative analysis starting from the evaluation of the antibacterial activity of the two antimicrobial peptides deriving from animal sources displayed a spectrum of action against Gram-positive bacteria. This observation of specificity towards *S. aureus ATCC25923* promote the testing of the two antimicrobial peptides regarding their antibiofilm properties. Currently, biofilm-related inflection

represents a relevant clinical problem because of the intrinsic recalcitrance of the biofilm to the antibiotic therapy. *S. aureus* is a common bacterial species involved in biofilm-associated infections such as implant-related infections, wound healing etc. When assayed against preformed biofilm temporin B and BmKn2 were able to reduce the biofilm at the concentration of 25µg/ml and a complete eradication at 50µg/ml as shown in Figure 11, results obtained by colony counting. It is commonly recognized that preformed biofilms are more challenging to eradicate rather than early stage of biofilm formation, revealing in this case a good antibiofilm activity of both antimicrobial peptides. As bacteria within mature biofilm are less sensitive to antibacterial agents than log-phase bacteria, the activity of the two antimicrobial peptides was obtained for the 2h hour old biofilm. Temporin B treatment caused a reduction of >50% of the preformed biofilm at 25µg/ml and 100% complete eradication of the preformed biofilm at 50µg/ml. Same results were obtained with BmKn2, showing a reduction of almost 50% of the preformed biofilm and 100% eradication at 50µg/ml.

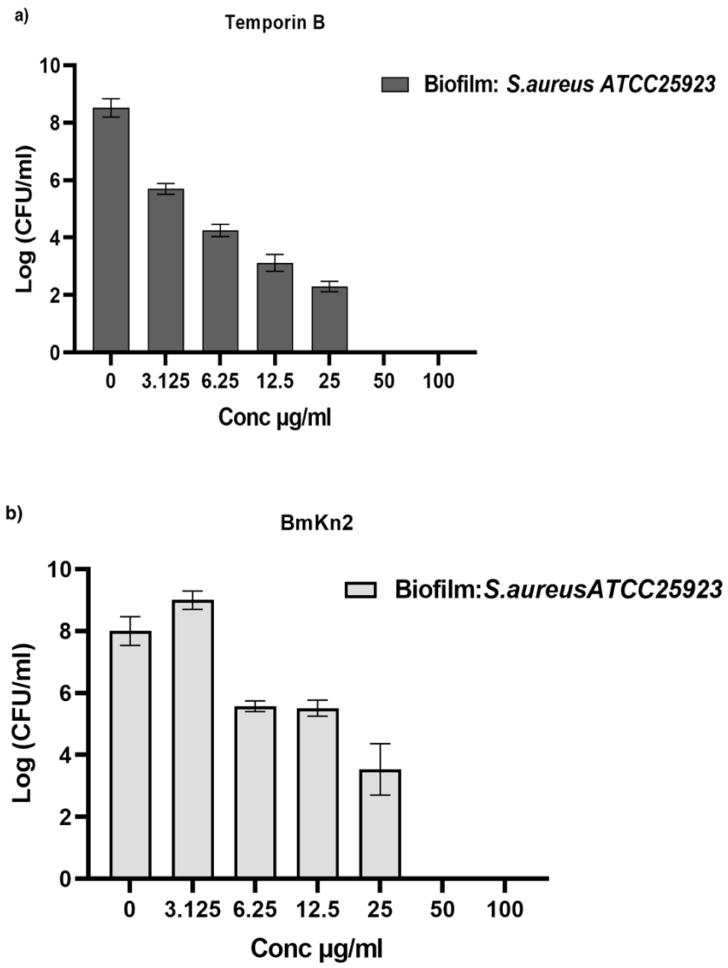


*Fig 11. Antibiofilm activity against 24 h-old, preformed biofilm of S. aureus ATCC25923. The biofilm surviving the treatment of **a)** temporin B and **b)** BmKn2 were enumerated by CFU count. Data are expressed as the $Log_{10}$ CFU/ml of untreated bacteria (control) and antimicrobial peptides treated bacteria (sample).*

## 3.2. Mesoporous silica nanoparticles as AMPs drug delivery

Mesoporous silica nanoparticles were synthetized and used as drug delivery system for the antimicrobial peptides synthetized and tested above against antibacterial and antibiofouling activity. A sol-gel synthetic method was used to obtain mesoporous silica particles according to published procedure in section (Materials and methods). The mean pore size of the particles was about 2.5 nm as determined by nitrogen sorption analysis with BJH method. The specific surface area $S_{BET}$ was 1165 $m^2/g$ and pore volume 0.6 $cm^3/g$. The isotherm, shown in Figure 12 a, is a type IV (according to the IUPAC classification)[73]. Representative electron microscopy images of MSNs are shown in figure 12. Particle size, obtained from SEM images (ImageJ software), shows a monodisperse distribution centered at 85 nm (see Figure 12 b).

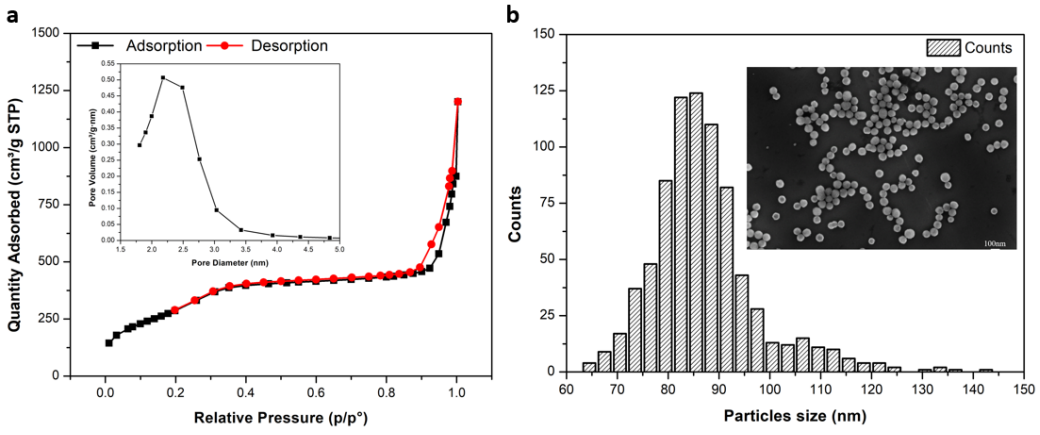


*Fig 12. a) Nitrogen Sorption Isotherm and size pores of MSNs and (**b**) Dimensional analysis from SEM images.*

The adsorption of the antimicrobial peptides was carried out in PBS buffer, with best adsorption at pH 10. The amounts of temporin B and BmKn2 adsorbed into silica material are expressed in terms of drug loading capacity (LC%) so defined:

$$\mathrm{LC}(\%) = \frac{\mathrm{drug_{added}} - \mathrm{drug_{free(not\ entrapped)}}}{\mathrm{drug_{added}}} \mathrm{x}\ 100$$

LC% is calculated based on the peptide concentration.

The cumulative release ($C_r$) is calculated based on the following formula:

$$\mathrm{C_r} = \frac{\mathrm{drug_{free}}}{\mathrm{drug_{total}}} \mathrm{x}\ 100$$

where total drug is the initial amount of drug encapsulated into mesoporous silica and drug free is the amount of drug released in the supernatant determined, using the described analytical procedure by RP-HPLC. Both, loading and kinetic release are dependent on the pH of the medium (Table 2).

**Table 2.** Loading and release properties of mesoporous silica based on pH.

| Materials | Load (LC%) | Release (%) |
|---|---|---|
| **Temporin B – MSNs pH 10** | 86.0 ± 1.2 | 0 |
| **Temporin B – MSNs pH 7.4** | 37.0 ± 1.6 | 8.0±2.5 |
| **Temporin B – MSNs pH 5.5** | 0 | 81±1 |
| **BmKn2 – MSNs pH 10** | 90.5±4.9 | 0 |
| **BmKn2– MSNs pH 7.4** | 42.0±3 | 10.0±0.4 |
| **BmKn2– MSNs pH 5.5** | 0 | 89.0±0.05 |

The adsorption and the release of the analysed peptides is pH dependent: high pH favour the loading of peptides in MSNs instead low pH favour their release. BmKn2 has a better adsorption compared to temporin B 0.45 mg/ml and 0.42 mg/ml respectively in 1 mg/ml of mesoporous silica nanoparticles at the higher tested pH 10 (Figure 14). Considering the estimated volume of temporin B (1680 $Å^3$) and BmKn2 (1700 $Å^3$) the overall volume of peptides loaded into mesoporous silica can be estimated at approximately 0.3 and 0.33 $cm^3/gr$ respectively which is compatible with the porosity of nanoparticles of 0.6 $cm^3/gr$. Since the size of both peptides is about 2nm **(**Figure 13), less than the porosity diameter, we hypothesize that peptides are largely adsorbed within porosity.

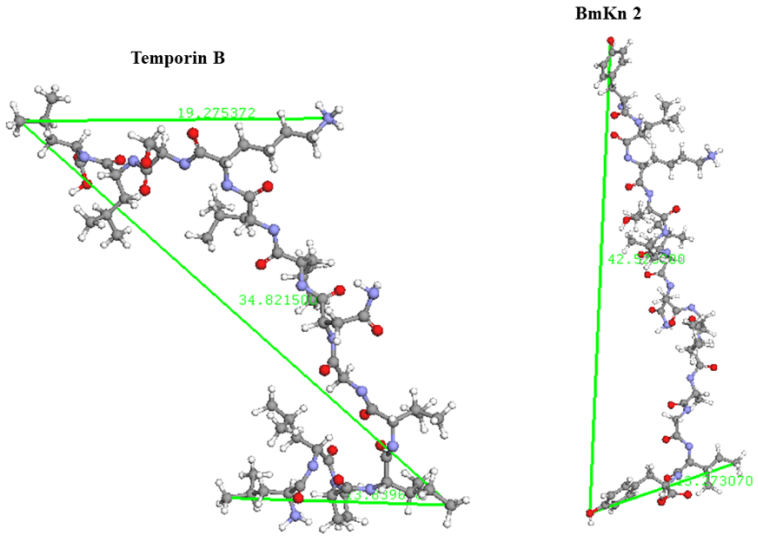


*Fig 13. 3D representation of the antimicrobial peptides studied with sizes around 2nm.*

The peptides have their appreciable release within 24 hours, up to 0.35 mg/ml for temporin B (83% of the loaded peptide) instead BmKn2 showed a release up to 0.40 mg/ml (89% of the loaded peptide) at the lower tested pH 5.5.

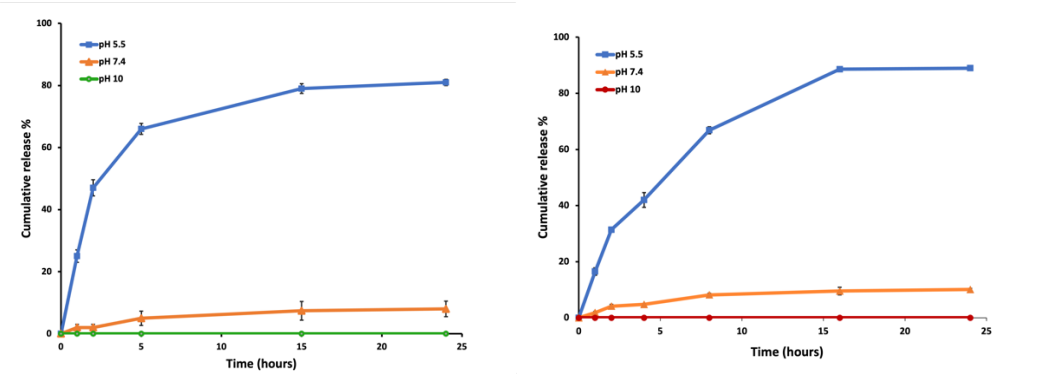


*Fig 14. Release profiles from mesoporous silica nanoparticles of temporin B, left graph and BmKn2 right graph, showing the influence of the pH on the release of both antimicrobial peptides.*

The pH dependence of loading and release of these peptides can be explained by the different behaviour of mesoporous silica and peptides: while silica becomes more negative as the pH increases and the peptides temporin B and Bmkn2 are still positively charged (Figure 15).

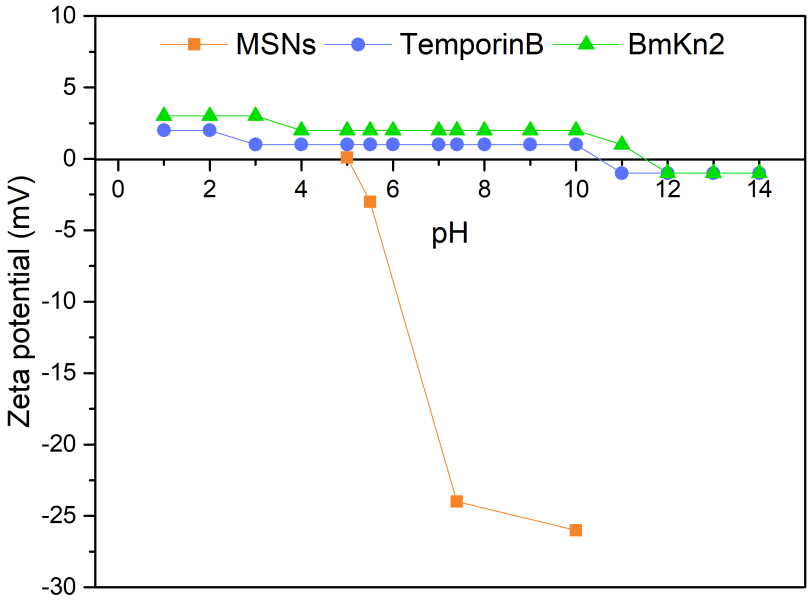


*Fig 15. Zeta potential profile of MSNs in different pH ranges (experimental data), and the charges of the antimicrobial peptides at different pH calculated with [www.pepdraw.com](http://www.pepdraw.com)*

BmKn2 compared to temporin B present two positive charges, and this explain its highest adsorption concentration into the negatively charged MSNs.

The observed release at pH 7.4 is low (close to 10%) for the studied peptides so a large amount of AMPs may be preserved in MSNs during circulation in physiological environment (pH 7.4) while upon arrival in infection sites more drug will be released under triggered by acidic signals in specific pathological acidic environment of infections. Moreover, the pH sensitivity of MSNs samples is expected to increase selectivity of the drug delivery to infection sites with a more precise and controllable release strategy and less toxicity than concentration-dependent diffusion reducing the rate of peptide release in normal space.

The antibacterial activity of temporin B and BmKn2 loaded MSNs further was explore in vitro against S. aureus ATCC25923. A starting inoculum of 1 x $10^6$

CFU/ml and a concentration of 133 µg/ml of temporin b and 50µg/ml of BmKn2 loaded into the MSNs with a serial dilution corresponding to 1 µg/ml of final concentration. Same conditions were used for the free peptides, in order to have the same amount of peptide released from the carrier, according to the release data. Bacteria incubated in the medium assay only served as control of cell-viability. AMPs loaded MSNs exerted same antibacterial activity in terms of minimum inhibition concentration (16 µg/ml for temporin B and 6.25µg/ml for BmKn2) of the free peptide showing an entirely inhibition of S. aureus ATCC25923. Meanwhile, there is no antibacterial activity observed upon the concentration of empty mesoporous silica carrier up to 175 µg/ml. Figure 16 shows the curves generated by UV absorbance at 600 nm (optical density OD), related to the minimum inhibition activity.

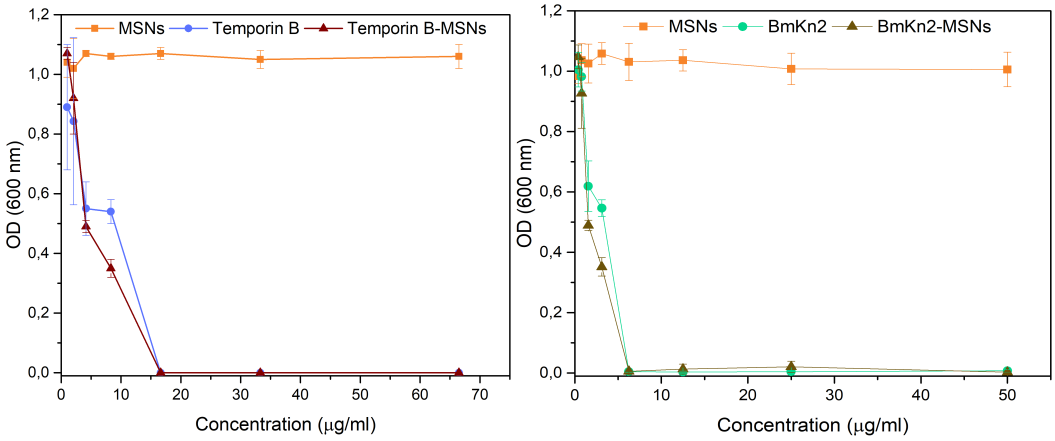


*Fig 16. Antibacterial activity of temporin B (left) and BmKns (right) tested alone and loaded to the mesoporous silica nanoparticles.*

These results show that the antimicrobial peptides activity in conserved after being adsorbed and then released by silica nanoparticles.

Temporin B – MSNs was further selected to evaluate the activity against S. aureus ATCC25923 biofilm formed on Calgary pegs device. As observed in figure 17 biofilm treated with temporin free and temporin B loaded MSNs determine an effective minimum biofilm eradicating concentration equal for both at 50 µg/ml, where no colonies were detected after treating 24 h-old biofilm. Again, we did not detect any inhibition or eradication of staphylococcal biofilm if treated with different concentration of empty mesoporous silica carrier (concentration reaching 175 µg/ml).

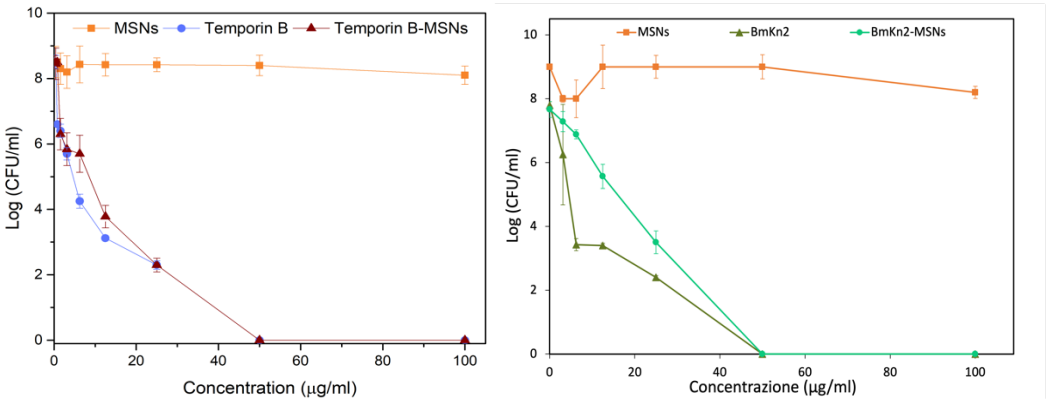


*Fig 17. Antibiofilm effect of temporin B (left) and BmKn2 (right) against S. aureus ATCC25923. Both antimicrobial peptides were tested alone and loaded with MSNs as drug delivery system. MBEC is conserved even when the AMPs are loaded into MSNs.*

Verified that mesoporous silica can be effectively used as carriers, at least for the analyzed antimicrobial peptides, we further investigate its ability to protect against degradation in order to deliver to the site of action the peptide in its active form. The stability of the peptides in the presence of proteases was assessed by incubation of free peptide for 10 min, 30 min and 60min, instead the peptides loaded MSNs

for 4, 8 and 16 hours at 37°C. Chromatographic analysis of free peptides show that are cleaved at multiple sites, resulting in a rapid degradation.

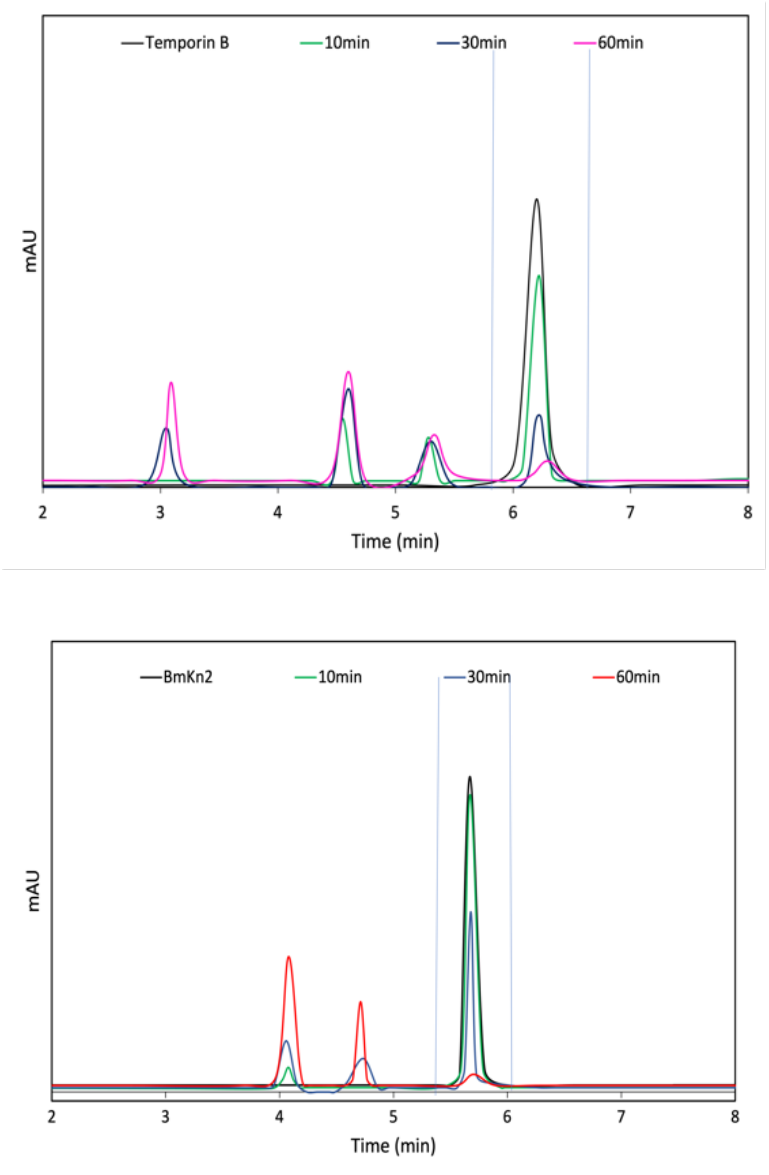


*Fig 18. Temporin B and BmKn2 HPLC chromatograms after treatment with enzyme proteinase K, without any drug delivery systems.*

In AMPs – MSNs the degradation was not observed, we hypothesize the mechanism in which the peptides are protected into the silica pores where the proteinase K

cannot reach due to the bigger size of the enzyme compared to the pores, so access of proteases may be sterically hindered. In the moment when milli-Q with 0.1% of TFA is added to the solution in presence with temporin B – MSNs or BmKn2 – MSNs the enzyme is unfolded causing loss of activity and the peptide is released because of pH decreasing.

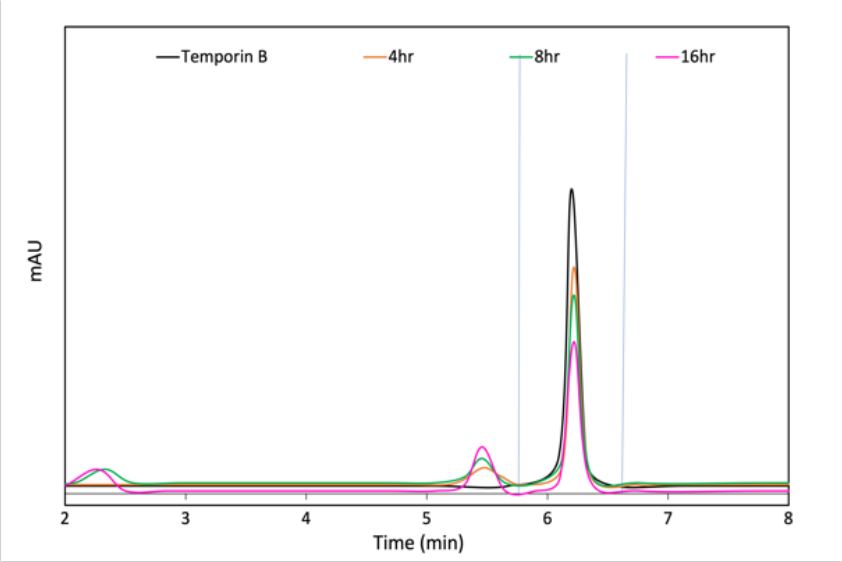


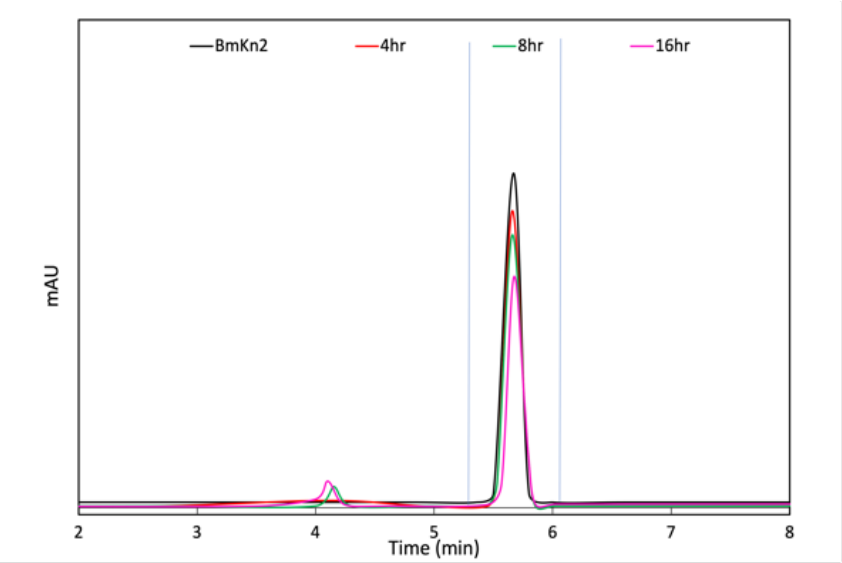


*Fig 19. Temporin B and BmKn2 loaded mesoporous silica nanoparticles chromatograms incubated with proteinase K enzyme. The antimicrobial peptides loaded MSNs are protected from the enzyme degradation.*

As is shown in figure 19 the peptide is not degraded after 16 hours, due to the protection from the mesoporous silica, and just the little amount of the peptide released (as shown for PBS pH 7.4) is cleaved from the enzyme. Instead, the free

peptide shows a very fast cleavage from the enzyme only after 10min of reaction and after 1 hour the peptide is almost totally degraded.

The cytotoxicity was examine of the tested antimicrobial peptides, against mammalian cells MRC5. As Shown in figure 20, BmKn2 shows a decrease in viability at higher concentration with an IC50 of 209$\mu$g/ml, instead this peptide loaded int o mesoporous silica nanoparticles shown an increase in cell viability, in demonstration that MSNs reduce the toxicity of the peptide, due also to the controlled release into the media. Is possible to observe the same reduction of toxicity even for temporin B, but in this case the viability of mammalian cells is higher even when the peptide solo.

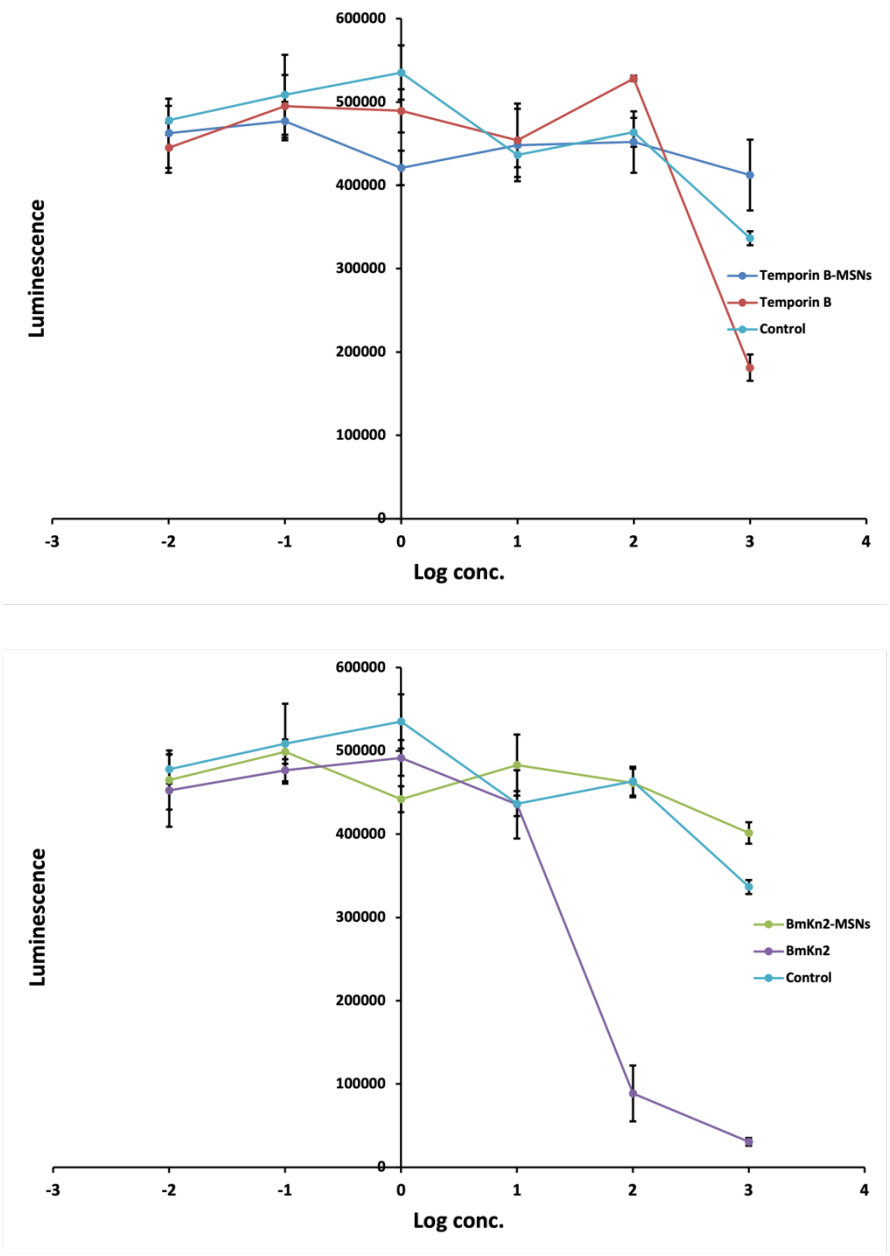


*Fig 20. Dose-dependent cytotoxycity of MRC5 treated with (up) BmKn2, BmKn2-MSNs and (down) Temporin B, Temporin B-MSNs*

## 3.3. Mesoporous zirconia nanoparticles as antibiotic drug delivery system

Mesoporous zirconia nanoparticles synthesis with regular shape and controlled size was performed using neutral surfactant assisted sol-gel method with NaF as inorganic salt. As described above a hydrothermal treatment followed the synthesis to define the shape of the nanoparticles and remove the traces of surfactant under vacuum, to avoid the collapse of pore which are crucial for a higher surface area and a higher drug loading.

FE-SEM analysis shows spherical nanoparticles with a mean diameter of 390±100 with a well-defined shape as shown in figure 21.

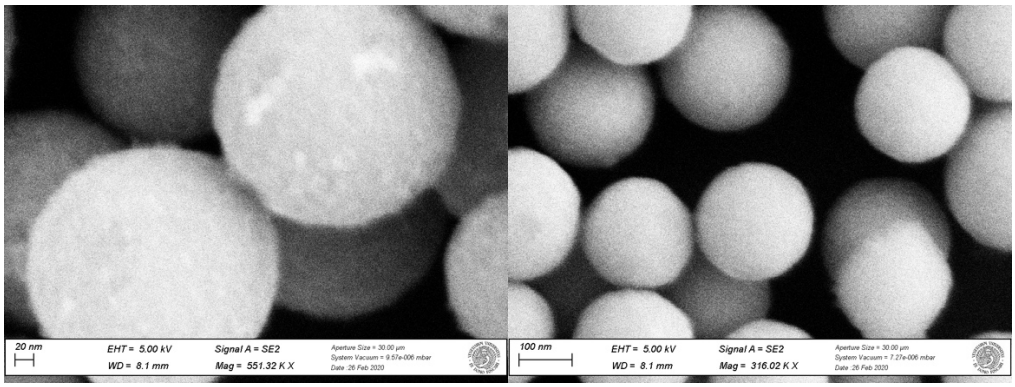


*Fig 21. FE-SEM images of mesoporous zirconia nanoparticles, on the left image the nanoparticles appear roughness, most probably because of the porosity of the nanoparticles with a diameter ~5nm as measured by BJH below. Instead, the right image exhibits the uniformity in shape and dimension of the nanoparticles.*

Nitrogen adsorption-desorption isotherm present type IV profile based on the "Brunauer classification" with a H1 hysteresis loop typical of mesoporous materials in accordance and IUPAC classification (Figure 22).

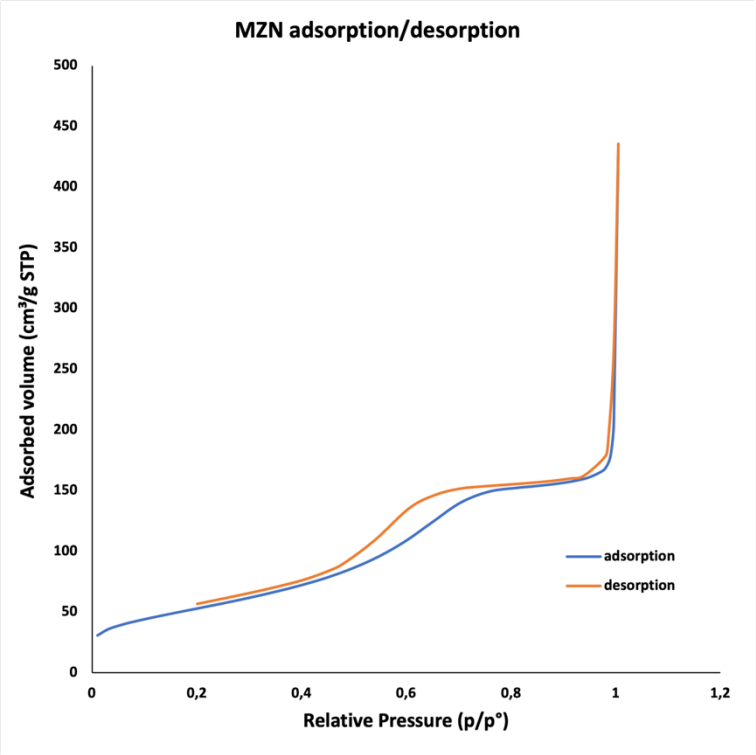


*Fig 22. $N_2$ adsorption/desorption of MZNs with an isotherm of type IV based on Brunauer classification and typical of mesoporous materials.*

The surface area of MZNs synthetized present an average of 215 $m^2/g$ and an average pore diameter of 5.3 nm according to BJH model applied, and with a pore volume of 0.26 $cm^3/g$. In figure 23 is represented the pore diameter of MZNs.

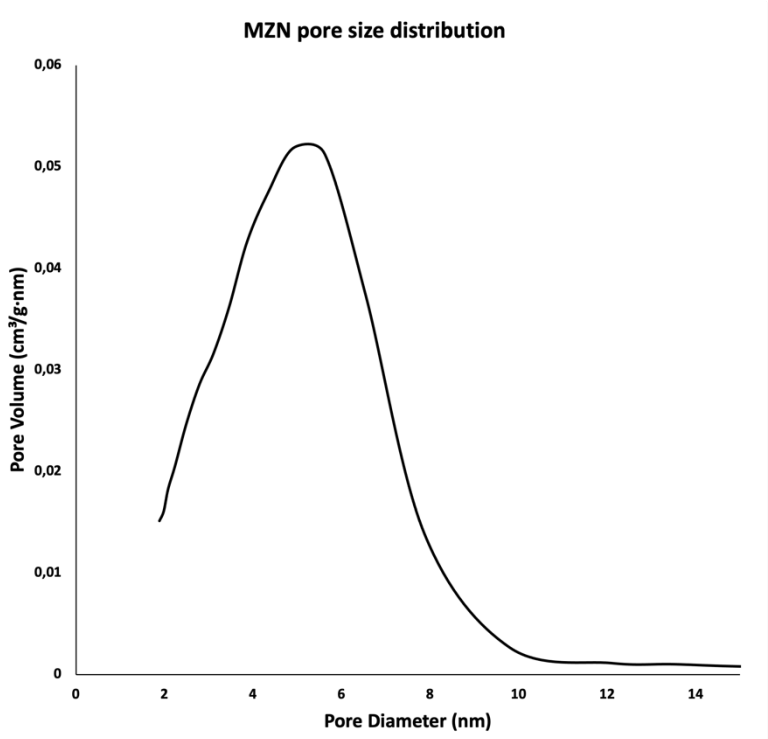


*Fig 23. Pore diameter of MZNs.*

After the characterization of MZNs by FE-SEM, BET and BJH loading of the antibiotic daptomycin into MZNs was performed. As reported [22]the superficial charge of the MZNs is dependent on the pH of the solution, which is very important to investigate before loading the drugs into the nanoparticles. MZNs is positive in acidic pH, with a neutral point ~6.5 -7 and negative at higher pH then the neutral point.

Daptomycin has an isoelectric point of ~4.8 which means below this value is positive and above is negative. The loading was performed in phosphate buffer saline at three different pH 5, 7.4 and 9. the loading was calculated based on nanoparticles amount and based on the antibiotic amount, which represent loading content and loading efficacy respectively as shown below by the formulas 1 and 2.

$$\%\ loading\ efficacy = \frac{drug\ loaded}{drugfree} x100 \qquad 1)$$

$$\%loading\ content = \frac{drug\ loaded}{amout\ NPs}\ x\ 100 \qquad 2)$$

Daptomycin loaded more at PBS pH 5 accordingly with the zeta potential of MZNs and isoelectric point of the antibiotic, the loading efficacy reaches a plateau at about 83% and 41,5% of loading content, calculated based on the amount of MZNs as described in the methods **(**figure 24). The loading was normalized to 83% as 100%, considering the washing away of any excess of the drug non loaded. At physiological pH 7,4 the loading efficacy is ~52% (and a loading content of 26%), in which MZNs is very closed to the neutral point, suggesting different interaction with the antibiotic rather than electrostatic interaction which are the main driving force of MZNs and daptomycin at pH 5.

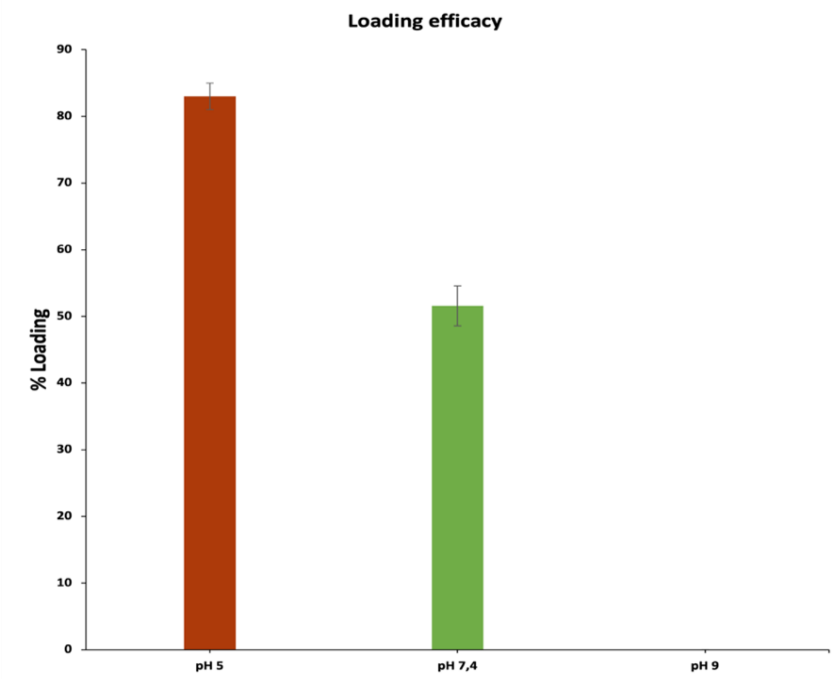


*Fig 24. Loading efficacy of daptomycin into mesoporous zirconia nanoparticles at different pH values.*

The loading at pH 5 was then used to perform the release of daptomycin from MZNs, and even in this case pH 5, 7.4 and 9 were tested. At pH 5 MZNs did not show any release, as shown in figure 24.

Regarding releases at pH 7,4 and 9 after 24 hours the release reaches a plateau for both samples. At pH 5 around 94% of daptomycin is released after 24 hours of shaking 150rpm at room temperature.

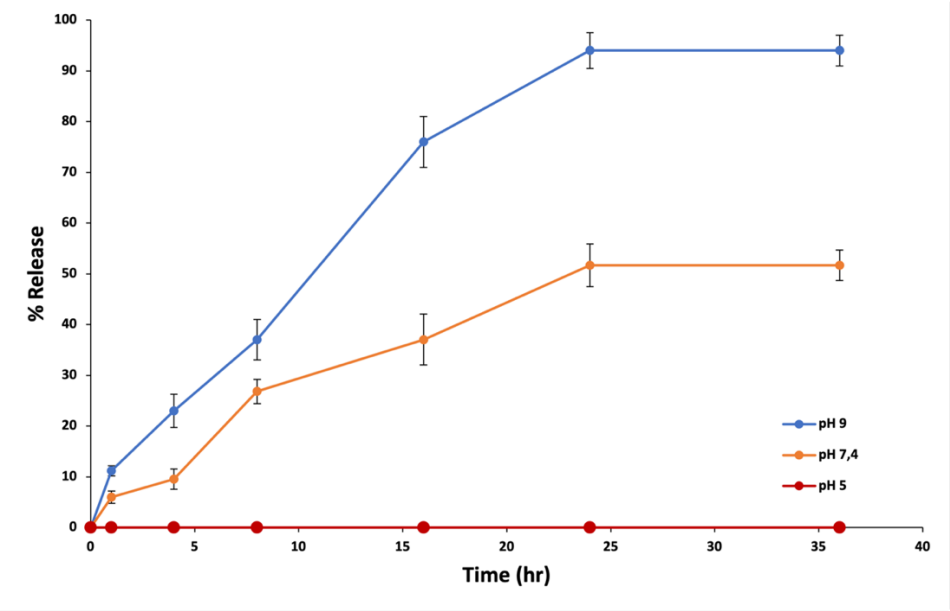


*Fig 25. Release profiles of daptomycin from MZNs, at different pH values.*

The results were verified three times in duplicate to ensure the amount of loading and release (Figure 25).

The mesoporous zirconia nanoparticles where then loaded and quantified to perform the *in vitro* antibacterial (planktonic) and antibiofilm activity. The *in vitro* determination of MIC of MZNs loaded the antibiotic daptomycin was performed as described in methods. The MICs obtained by microplate dilution test for daptomycin were consistent with the MIC of the antibiotic reported elsewhere[74] about 3.6µg/ml with a serial dilution starting from 28.9µg/ml to 0 for daptomycin. MZNs solo was tested against the strain *S. aureus ATCC25923* and the bacteria did not show any reduction in the range of concentrations used 200µg/ml to 0 (Figure 26).

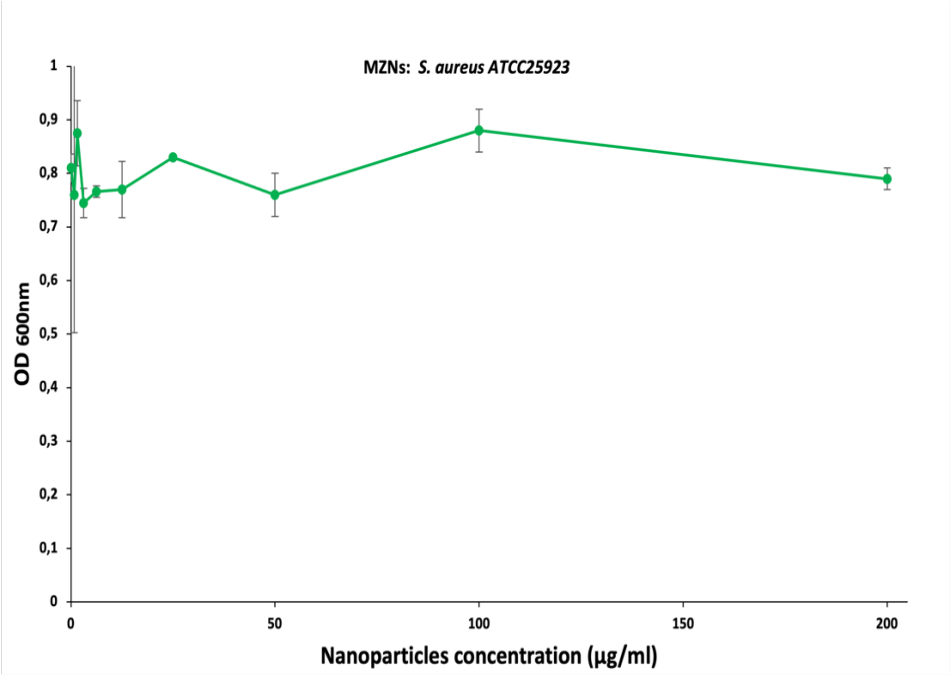


*Fig 26. Mesoporous zirconia nanoparticles tested against S. aureus ATCC25923, showing no antibacterial activity for the concentrations tested (200µg/ml to 0).*

Instead, MZNs loaded daptomycin, confirmed the results of daptomycin solo with a MIC of 3,6µg/ml and has the same trend as the drug free. The confirmation of the same MIC of daptomycin loaded MZNs is evidence that the released antibiotic retains its antibacterial activity during incubation with *S. aureus ATCC25923* for 24 hours (Figure 27). The turbidity of MZNs was subtracted from the final reading at 600nm, to avoid any false results.

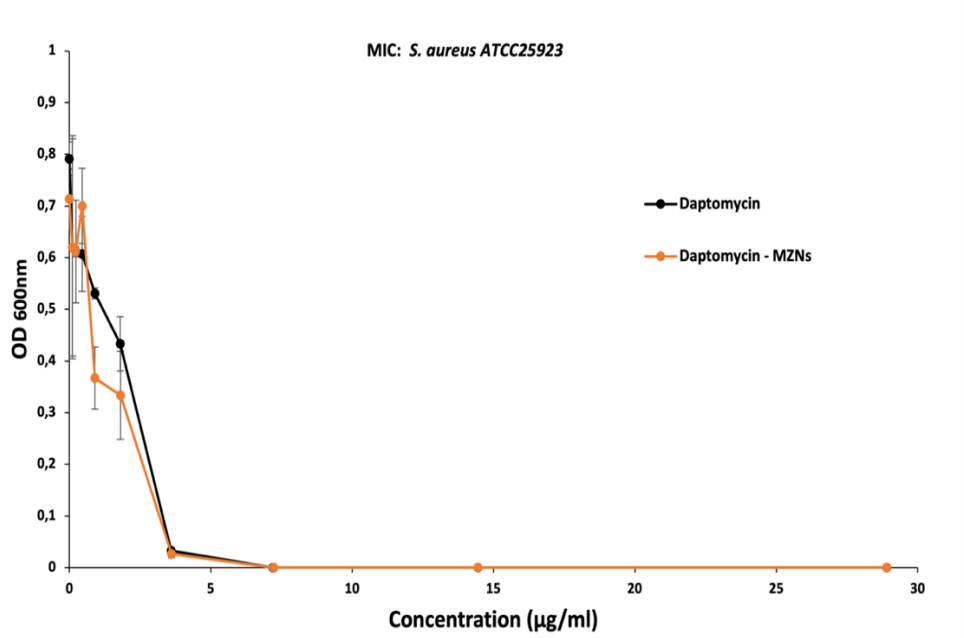


*Fig 27. S. aureus ATCC25923 growth inhibition treated with daptomycin solo and daptomycin loaded MZNs.*

After the antibacterial activity of daptomycin and daptomycin loaded MZNs was assessed antibiofouling activity was investigated. The antibiofilm activity was assessed by quantifying biofilm eradication using crystal violet (method used for time and practical reasons) stain. *S. aureus ATCC25923* cells were incubated for 24 hours to form biofilm and then treated with daptomycin solo and daptomycin loaded MZNs. Biofilms are characterized by their increased tolerance towards antibiotics, which has been demonstrated to increase the MBEC values of ten to 1,000-folds compared to MIC. The structure of biofilms together with the low metabolic activity of bacteria cells, is believed to be responsible for the increase of antibiotic tolerance. The penetration of antibiotics into biofilm may be hindered because of the multilayers of biofilm and the extracellular polysaccharides matrix. Since most antibiotics target the metabolic pathways of bacteria when their activity is decreased

leads to a prevention of antibiotic activity. Previous studies indicates that daptomycin shows good antibiofilm inhibition activity since daptomycin target is the cell membrane by opening pores and causing cell lysing. Regarding, daptomycin loaded MZNs the antibiofilm activity was totally conserved against eradication of preformed biofilm, which is challenge considering the above-described features of biofilm. MBEC, as shown in figure 28 is ~29µg/ml for both tested samples, comparable in terms of reliability with the MIC results of the system compared to the drug alone.

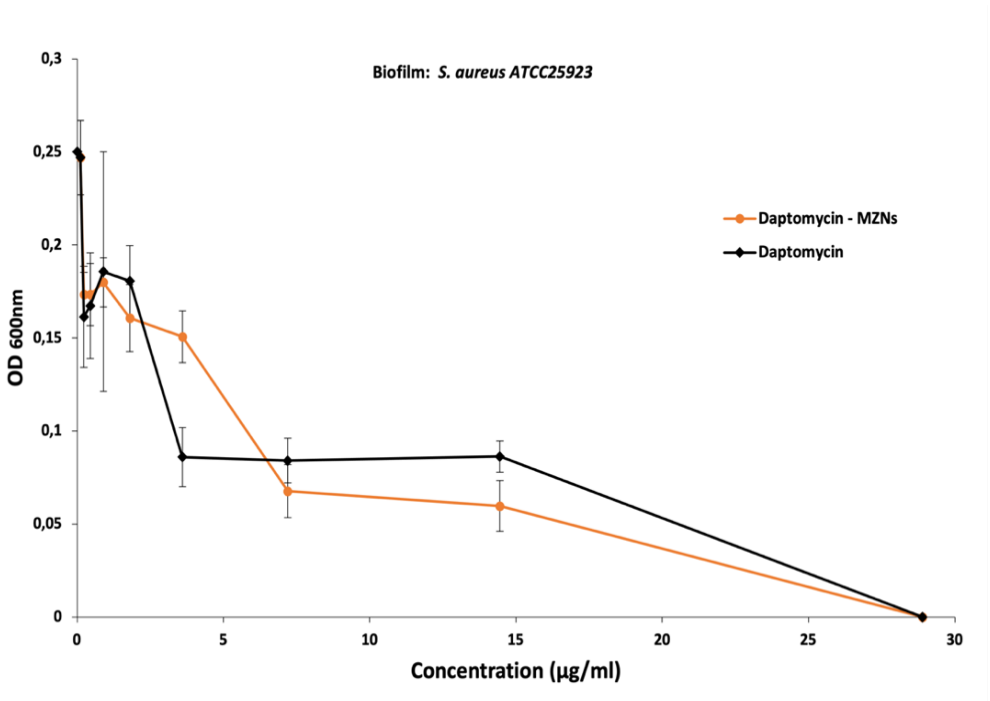


*Fig 28. Antibiofouling activity of daptomycin and daptomycin-MZNs.*

Using a well-established antibiotic as daptomycin against *S. aureus ATCC25923* to further study a delivery system as mesoporous zirconia nanoparticles in this study

was clearly shown that the antibiotic conserves its activity, and confirm the activity against preformed biofilm, which is known to be more resistant to antibiotics.

## 3.4. Amphiphilic polymer as antibiotic drug delivery system

Poly(acrylic acid) (PAA) macro-RAFT agent was synthetized by RAFT polymerization using methyl-2-(butylthiocarbonothioylthio)propanoate trithiocarbonate (MCEBTTC) as chain transfer agen. MCEBTTC was synthetized as reported in paper. The acrylic acid (AA) was initiated by AIBN and conducted in ethanol at 70°C. The polymerization kinetics was monitored by $^{1}$H-NMR, the spectrum of $^{1}$H-NMR of PAA macro-RAFT agent dissolved in DMSO-$d_6$ is illustrated in figure 29.

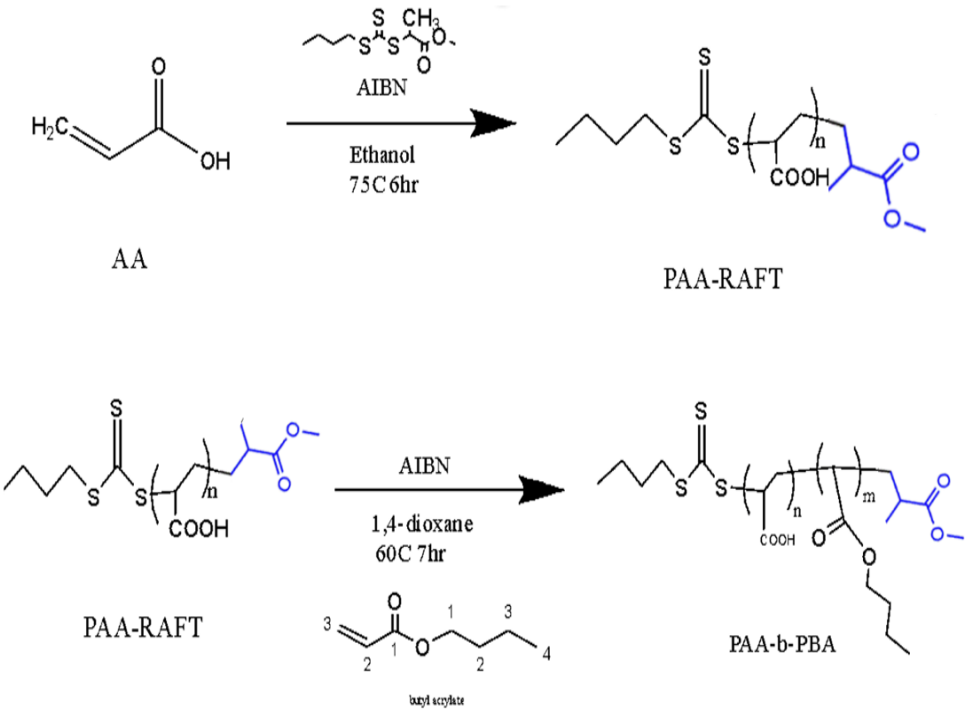


*Fig 29. Schematic representation of PAA-b-PBA synthesis.*

The $^{1}$H-NMR traces display a decrease of signals ~6.2 over time allowing to calculate the conversion of the monomer in macro-RAFT. The plot of $\ln([M]_0/[M]_t)$ as a function of time (*t* 10hr) displays a linear increase, indicating a pseudo-first-order kinetics.

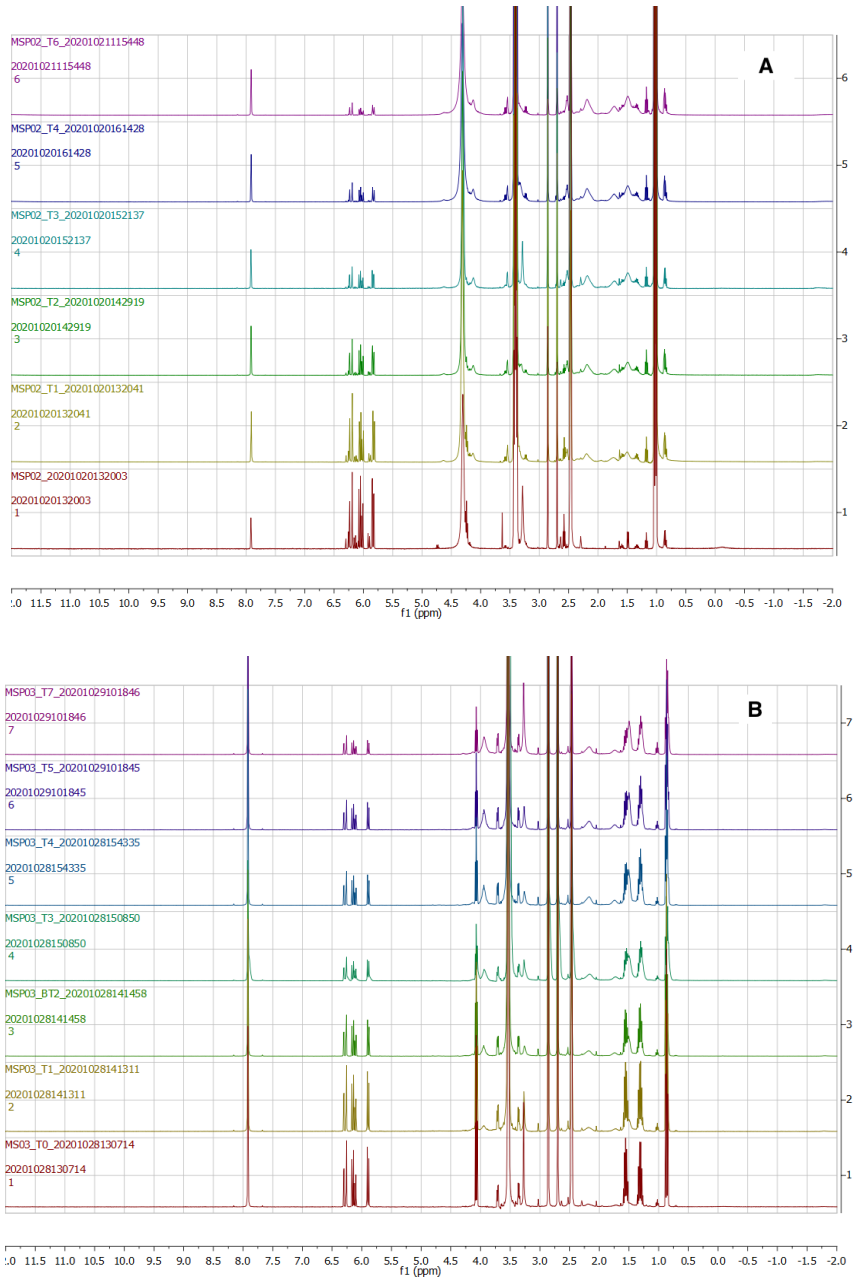


*Fig 30. NMR spectra's of macro RAFT (PAA macro-RAFT) synthesis and synthesis of PAA-b-PBA*

The successful polymerization of PAA macro-RAFT proven by $^{1}$H-NMR and GPC (Figure 30) allowed us to proceed with the synthesis of diblock copolymer PAA-*b*-PBA.

After precipitation and drying at 40°C overnight PAA macro-RAFT was solubilized in dioxane**.** The PAA macro-RAFT can be further chain extended with monomer butyl acrylate in dioxane to form the amphiphilic block copolymer able to self-assemble in water into micelles following the synthesis.

Monomer butyl acrylate conversion kinetics to PAA-*b*-PBA was again monitored by $^{1}$H-NMR for 7 hr. The polymerization of the block copolymer reaches a conversion of ~ 70%.

After the polymerization PAA-*b*-PBA was precipitated, dried at 40°C overnight, solubilized in milli-Q water and freeze-dried in order to remove any trace of solvents in order to use the amphiphilic block copolymer for the loading of antibiotic daptomycin.

Daptomycin is loaded into the amphiphilic polymer PAA-*b*-PBA, in the following concentrations 1mg/ml of daptomycin into 2mg/ml of the polymer, which represent the best ratio for the loading in PBS physiological pH. The sample is stirred with a magnetic stirrer into a glass vial overnight to allow the polymer to load the drug. After the loading the solution is placed in a dialysis bag in PBS medium, same conditions as for the loading in order to remove the non-loaded antibiotic overnight and measured at 260nm UV-visible, to calculate the effective loading of the drug. 85% of the antibiotic was loaded into the polymer and was then released in PBS pH 6 for 48 hours, showing as in figure 31 a gradual and slow release of daptomycin in acid condition. The release after 50 hours is about 93% of the amount of the antibiotic loaded.

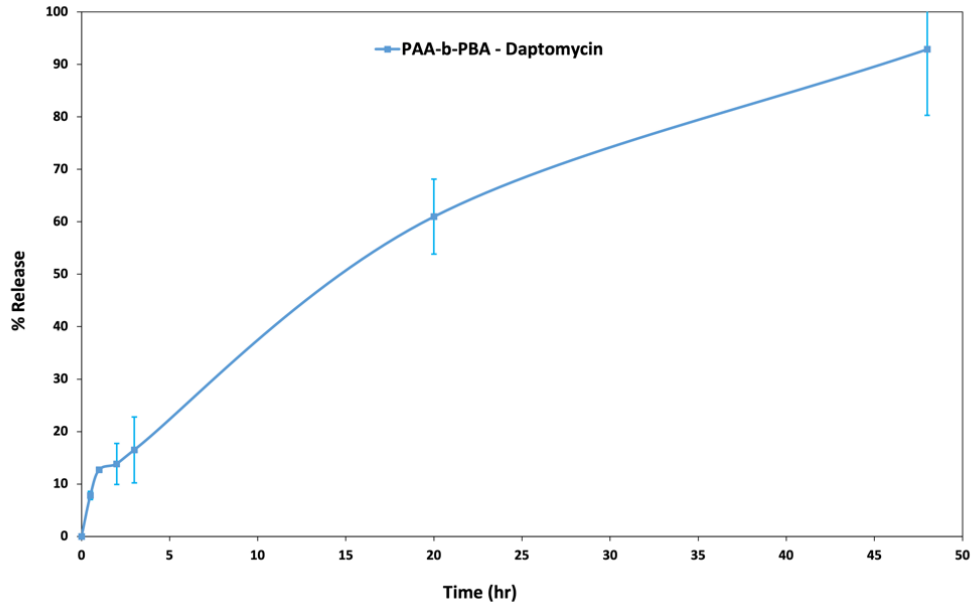


*Fig 31. Release profile and loading of daptomycin into the amphiphilic polymer PAA-b-PBA.*

Once the loading and release was settled, daptomycin loaded PAA-*b*-PBA was then tested against planktonic *S. aureus ATCC25923*. As shown in figure 32 PAA-*b*-PBA does not present any antibacterial activity against *S. aureus ATCC25923,* instead daptomycin and daptomycin loaded the polymer follow the same antibacterial activity as the antibiotic solo, confirming the inertness of the polymer and the conservation of the antibiotic activity after being released from the carrier entirely.

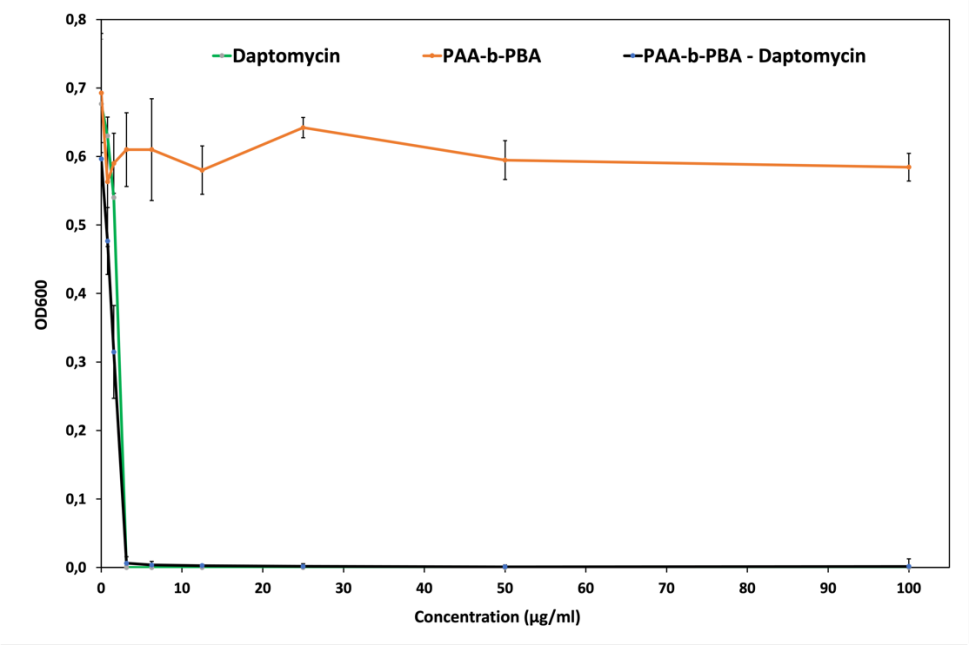


*Fig 32. Antibacterial activity of daptomycin solo, PAA-b-PBA solo and daptomycin loaded PAA-b-PBA showing the conservation of the antibiotic solo activity against* S. aureus ATCC25923.

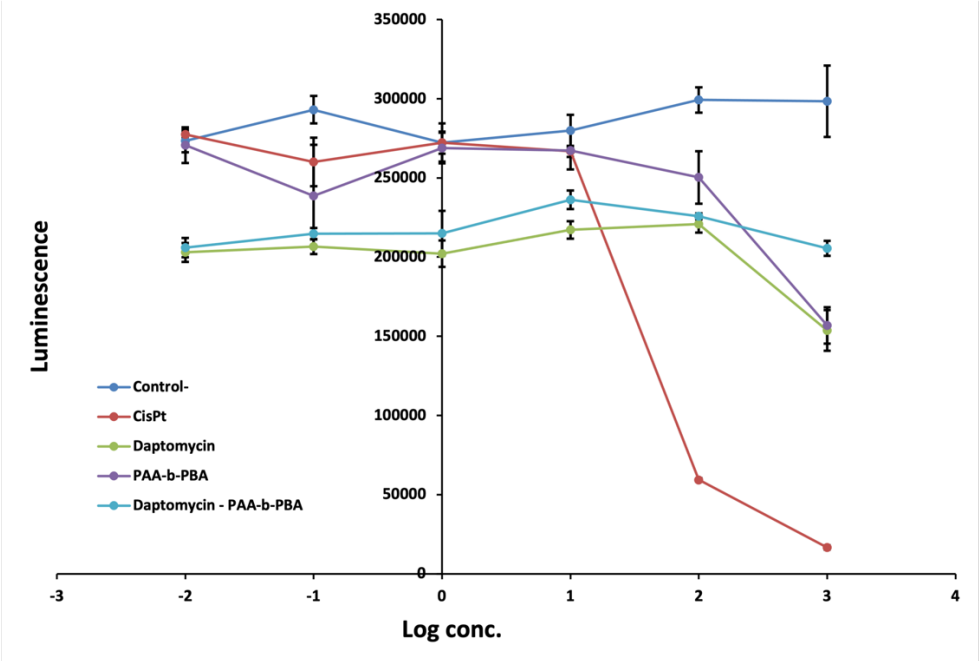


*Fig 33. Cytotoxicity test of the synthetized polymer and of the polymer loaded daptomycin*

Cytotoxicity of the polymer, daptomycin and the polymer loaded daptomycin was assessed against MRC5 cells. As shown in figure 33, no cytotoxic effect of is observed as with the positive control of CisPt at higher concentrations. The samples did not exhibit significant toxic effect against mammalian cells, at least not at concentrations lower than 1mg/ml, with represent a higher concentration compared with the highest concentration tested against bacteria which is 100µg/ml.

# 4. Conclusions

In the present work we have approached diverse drug delivery agents to investigate their features in delivering antimicrobial peptides and antibiotic daptomycin against *Staphylococcus aureus ATCC2529*.

In the first part antimicrobial peptides were synthetized and tested against bacterial and biofilm of gram-positive and gram-negative bacteria, showing better activity against gram-positive bacteria in ranged below 10µg/ml for planktonic and below 50µg/ml against biofilm.

Mesoporous silica nanoparticles were synthetized with the purpose to deliver and protect AMPs from enzymatic degradation. AMPs are very susceptible to enzyme degradation, which represent one of the limiting steps in the development of peptides as therapeutic agents. MSNs showed very good delivery and protection ability for AMPs temporin B and BmKn2, improving the stability of the peptides when incubated with proteinase K compared to the peptides solo.

Daptomycin was selected as antibiotic and cyclic peptides, and is a clinical antibacterial drug used against gram-positive infections.

Mesoporous zirconia nanoparticles, with bigger pores then MSNs were synthetized and loaded with daptomycin in order to investigate the loading and release capacity and evaluate the conservation of the antibacterial activity. The system showed good stability and antibacterial/antibiofilm activity against *Staphylococcus aureus ATCC2529* as an inorganic drug carrier for antibacterial drugs.

Amphiphilic polymer PAA-*b*-PBA was synthetized and loaded with daptomycin to investigate the ability as an organic nanocarrier for daptomycin. The polymer

showed good loading of the drugs and a slow release of daptomycin in acidic conditions, in which the polymer releases the antibiotic. Antibacterial activity of daptomycin were entirely conserved after loading into the polymer in ranges below 10μg/ml as the daptomycin solo.

Cytotoxic test *in vitro* confirmed the non-toxic effect of mesoporous silica nanoparticles and reduced the toxicity of BmKn2 when loaded to the nanoparticles. PAA-*b*-PBA did not show any cytotoxic effect, resulting as a suitable organic nanocarrier not just for antibacterial delivery.

In summary, we investigated deeply the properties of inorganic and organic drug delivery systems for antimicrobial agents. These properties make these drug delivers powerful nano-agents in theragnostic applications. While the high efficacy of these nanoparticles in antimicrobial delivery has been demonstrated *in vitro*, it would be highly desirable to extend these strategies to future *in vivo* studies.

# References


1. Quan, C.-Y. *et al.* Core−Shell Nanosized Assemblies Mediated by the α−β Cyclodextrin Dimer with a Tumor-Triggered Targeting Property. *ACS Nano* **4**, 4211–4219 (2010).
2. Torchilin, V. P. Recent advances with liposomes as pharmaceutical carriers. *Nat. Rev. Drug Discov.* **4**, 145–160 (2005).
3. Discher, B. M. *et al.* Polymersomes: Tough Vesicles Made from Diblock Copolymers. *Science (80-. ).* **284**, 1143–1146 (1999).
4. Niculescu, V. C. Mesoporous Silica Nanoparticles for Bio-Applications. *Frontiers in Materials* vol. 7 (2020).
5. Sponchia, G. *et al.* Biocompatible tailored zirconia mesoporous nanoparticles with high surface area for theranostic applications. *J. Mater. Chem. B* **3**, 7300–7306 (2015).
6. Li, W. *et al.* High drug-loaded microspheres enabled by controlled in-droplet precipitation promote functional recovery after spinal cord injury. *Nat. Commun.* **13**, 1262 (2022).
7. Rossi, F., Sharon, M., Irudayaraj, J., Vega-Vásquez, P. & Mosier, N. S. Nanoscale Drug Delivery Systems: From Medicine to Agriculture. *Front. Bioeng. Biotechnol.* | *www.frontiersin.org* **8**, 79 (2020).
8. Liu, Y. *et al.* Formulation of Nanoparticles Using Mixing-Induced Nanoprecipitation for Drug Delivery. *Ind. Eng. Chem. Res.* **59**, 4134–4149 (2020).
9. Huynh, C. T. & Lee, D. S. Controlled Release. in *Encyclopedia of Polymeric Nanomaterials* 439–449 (Springer Berlin Heidelberg, 2015). doi:10.1007/978-3-642-29648-2_314.
10. Adepu, S., Ramakrishna, S., Costa-Pinto, R. & Oliveira, A. L. molecules Controlled Drug Delivery Systems: Current Status and Future Directions. (2021) doi:10.3390/molecules26195905.

11. Park, H., Otte, A. & Park, K. Evolution of drug delivery systems: From 1950 to 2020 and beyond. *J. Control. Release* **342**, 53–65 (2022).

12. Zuccari, G. *et al.* Mini-Tablets: A Valid Strategy to Combine Efficacy and Safety in Pediatrics. *Pharmaceuticals* **15**, 108 (2022).

13. Wais, U., Jackson, A. W., He, T. & Zhang, H. Nanoformulation and encapsulation approaches for poorly water-soluble drug nanoparticles. *Nanoscale* **8**, 1746–1769 (2016).

14. Schoenmaker, L. *et al.* mRNA-lipid nanoparticle COVID-19 vaccines: Structure and stability. *Int. J. Pharm.* **601**, 120586 (2021).

15. *Lasting impact of lipid nanoparticles*. doi:10.1038/s41578-021-00398-6.

16. Patra, J. K. *et al.* Nano based drug delivery systems: recent developments and future prospects. *J. Nanobiotechnology* **16**, 71 (2018).

17. Senapati, S., Mahanta, A. K., Kumar, S. & Maiti, P. Controlled drug delivery vehicles for cancer treatment and their performance. *Signal Transduct. Target. Ther.* **3**, (2018).

18. Wang, Z., Hu, T., Liang, R. & Wei, M. Application of Zero-Dimensional Nanomaterials in Biosensing. *Front. Chem.* **8**, (2020).

19. Vallet-Regí, M., Colilla, M., Izquierdo-Barba, I. & Manzano, M. Mesoporous Silica Nanoparticles for Drug Delivery: Current Insights. *Molecules* **23**, 47 (2017).

20. Bharti, C. Mesoporous silica nanoparticles in target drug delivery system: A review. *Int. J. Pharm. Investig.* |, (2015).

21. Liu, X. *et al.* Article 598722 (2020) A Review of Mesoporous Silica Nanoparticle Delivery Systems in Chemo-Based Combination Cancer Therapies. *Front. Chem* **8**, 598722 (2020).

22. Leonetti, B. *et al.* Mesoporous zirconia nanoparticles as drug delivery systems: Drug loading, stability and release. *J. Drug Deliv. Sci. Technol.* **61**, 102189 (2021).

23. López-Dávila, V., Seifalian, A. M. & Loizidou, M. Organic nanocarriers for cancer drug delivery. *Curr. Opin. Pharmacol.* **12**, 414–419 (2012).

24. Begines, B. *et al.* Polymeric Nanoparticles for Drug Delivery: Recent Developments and Future Prospects. doi:10.3390/nano10071403.

25. Calzoni, E. *et al.* Biocompatible Polymer Nanoparticles for Drug Delivery Applications in Cancer and Neurodegenerative Disorder Therapies. *J. Funct. Biomater.* **10**, 4 (2019).

26. Zielińska, A. *et al.* Polymeric Nanoparticles: Production, Characterization, Toxicology and Ecotoxicology. *Molecules* **25**, 3731 (2020).

27. Bozzuto, G. & Molinari, A. Liposomes as nanomedical devices. *Int. J. Nanomedicine* 975 (2015) doi:10.2147/IJN.S68861.

28. Hanafy, N., El-Kemary, M. & Leporatti, S. Micelles Structure Development as a Strategy to Improve Smart Cancer Therapy. *Cancers (Basel).* **10**, 238 (2018).

29. Savić, R., Eisenberg, A. & Maysinger, D. Block copolymer micelles as delivery vehicles of hydrophobic drugs: Micelle–cell interactions. *J. Drug Target.* **14**, 343–355 (2006).

30. Reimhult, E. *et al.* Biomolecules Turn Self-Assembling Amphiphilic Block Co-polymer Platforms Into Biomimetic Interfaces. *Front. Chem.* | *www.frontiersin.org* **1**, 645 (2019).

31. Feng, H., Lu, X., Wang, W., Kang, N.-G. & Mays, J. Block Copolymers: Synthesis, Self-Assembly, and Applications. *Polymers (Basel).* **9**, 494 (2017).

32. Levit, M. *et al. Bio-Inspired Amphiphilic Block-Copolymers Based on Synthetic Glycopolymer and Poly(Amino Acid) as Potential Drug Delivery Systems*.

33. Moad, G. RAFT polymerization to form stimuli-responsive polymers. *Polym. Chem.* **8**, 177–219 (2017).

34. Ding, M., Zhao, W., Song, L.-J. & Luan, S.-F. Stimuli-responsive nanocarriers for bacterial

biofilm treatment. *Rare Met.* **41**, (2016).

35. Li, D. *et al.* Formulation of pH-responsive PEGylated nanoparticles with high drug loading capacity and programmable drug release for enhanced antibacterial activity. *Bioact. Mater.* **16**, 47–56 (2022).
36. Mura, S., Nicolas, J. & Couvreur, P. Stimuli-responsive nanocarriers for drug delivery. *Nat. Publ. Gr.* (2013) doi:10.1038/NMAT3776.
37. Balaure, P. C., Gudovan, D. & Gudovan, I. A. Smart Triggered Release in Controlled Drug Delivery. *Curr. Drug Targets* **19**, 318–327 (2018).
38. Chen, B. *et al.* Current Multistage Drug Delivery Systems Based on the Tumor Microenvironment. *Theranostics* **7**, 538–558 (2017).
39. Murray, C. J. *et al.* Global burden of bacterial antimicrobial resistance in 2019: a systematic analysis. *Lancet* **399**, 629–655 (2022).
40. Stewart, P. S. & William Costerton, J. Antibiotic resistance of bacteria in biofilms. *Lancet* **358**, 135–138 (2001).
41. Li, Y., Xiao, P., Wang, Y. & Hao, Y. Mechanisms and Control Measures of Mature Biofilm Resistance to Antimicrobial Agents in the Clinical Context. *ACS Omega* **5**, 22684–22690 (2020).
42. Tsuneda, S. *et al.* The Composition and Structure of Biofilms Developed by Propionibacterium acnes Isolated from Cardiac Pacemaker Devices. (2018) doi:10.3389/fmicb.2018.00182.
43. Archer, N. K. *et al. Staphylococcus aureus* biofilms. *Virulence* **2**, 445–459 (2011).
44. Neopane, P., Nepal, H. P., Shrestha, R., Uehara, O. & Abiko, Y. In vitro biofilm formation by Staphylococcus aureus isolated from wounds of hospital-admitted patients and their

association with antimicrobial resistance. *Int. J. Gen. Med.* 11–25 (2018) doi:10.2147/IJGM.S153268.

45. Nakatsuji, T. & Gallo, R. L. Antimicrobial Peptides: Old Molecules with New Ideas. *J. Invest. Dermatol.* **132**, 887–895 (2012).

46. Fleming, A. & lexander F leming, B. A. *Macmillan. (5) Gallavardin, ' La Tension arterielle en Clinique*. *Arch. f. exp. Path* vol. 4 https://royalsocietypublishing.org/ (1880).

47. Fleming, A. & lexander F leming, B. A. On a remarkable bacteriolytic element found in tissues and secretions. *Proc. R. Soc. London. Ser. B, Contain. Pap. a Biol. Character* **93**, 306–317 (1922).

48. Steiner, H., Hultmark, D., Engström, Å., Bennich, H. & Boman, H. G. Sequence and specificity of two antibacterial proteins involved in insect immunity. *Nature* **292**, 246–248 (1981).

49. Wollman, F.-A. An antimicrobial origin of transit peptides accounts for early endosymbiotic events. (2016) doi:10.1111/tra.12446.

50. Moretta, A. *et al.* Antimicrobial Peptides: A New Hope in Biomedical and Pharmaceutical Fields. *Article* **11**, 1 (2021).

51. Patocka, J., Nepovimova, E., Klimova, B., Wu, Q. & Kuca, K. Antimicrobial Peptides: Amphibian Host Defense Peptides. *Curr. Med. Chem.* **26**, 5924–5946 (2019).

52. Strömstedt, A. A., Ringstad, L., Schmidtchen, A. & Malmsten, M. Interaction between amphiphilic peptides and phospholipid membranes. *Curr. Opin. Colloid Interface Sci.* **15**, 467–478 (2010).

53. Brogden, K. A. Antimicrobial peptides: pore formers or metabolic inhibitors in bacteria? *Nat. Rev. Microbiol.* **3**, 238–250 (2005).

54. Pasupuleti, M., Schmidtchen, A. & Malmsten, M. Antimicrobial peptides: key components of the innate immune system. *Crit. Rev. Biotechnol.* **32**, 143–171 (2012).

55. Hancock, R. E. W. & Sahl, H.-G. Antimicrobial and host-defense peptides as new anti-infective therapeutic strategies. *Nat. Biotechnol.* **24**, 1551–1557 (2006).

56. Ringstad, L., Andersson Nordahl, E., Schmidtchen, A. & Malmsten, M. Composition Effect on Peptide Interaction with Lipids and Bacteria: Variants of C3a Peptide CNY21. *Biophys. J.* **92**, 87–98 (2007).

57. Singh, S., Kasetty, G., Schmidtchen, A. & Malmsten, M. Membrane and lipopolysaccharide interactions of C-terminal peptides from S1 peptidases. *Biochim. Biophys. Acta - Biomembr.* **1818**, 2244–2251 (2012).

58. Malmsten, M. Interactions of Antimicrobial Peptides with Bacterial Membranes and Membrane Components. *Curr. Top. Med. Chem.* **16**, 16–24 (2015).

59. Mohanram, H. & Bhattacharjya, S. 'Lollipop'-shaped helical structure of a hybrid antimicrobial peptide of temporin B-lipopolysaccharide binding motif and mapping cationic residues in antibacterial activity. *Biochim. Biophys. Acta - Gen. Subj.* **1860**, 1362–1372 (2016).

60. Marcocci, M. E. *et al. The Amphibian Antimicrobial Peptide Temporin B Inhibits In Vitro Herpes Simplex Virus 1 Infection*. https://doi.org/10 (2018).

61. Manzo, G. *et al.* Minor sequence modifications in temporin B cause drastic changes in antibacterial potency and selectivity by fundamentally altering membrane activity OPEN. doi:10.1038/s41598-018-37630-3.

62. Giacometti, A. *et al.* Interaction of Antimicrobial Peptide Temporin L with Lipopolysaccharide In Vitro and in Experimental Rat Models of Septic Shock Caused by

Gram-Negative Bacteria. *Antimicrob. Agents Chemother.* **50**, 2478–2486 (2006).

63. Carotenuto, A. *et al.* A Different Molecular Mechanism Underlying Antimicrobial and Hemolytic Actions of Temporins A and L. *J. Med. Chem.* **51**, 2354–2362 (2008).

64. Arpornsuwan, T., Buasakul, B., Jaresitthikunchai, J. & Roytrakul, S. Potent and rapid antigonococcal activity of the venom peptide BmKn2 and its derivatives against different Maldi biotype of multidrug-resistant Neisseria gonorrhoeae. *Peptides* **53**, 315–320 (2014).

65. Arpornsuwan, T. *et al.* Anticancer Activities of Antimicrobial BmKn2 Peptides Against Oral and Colon Cancer Cells. *Int. J. Pept. Res. Ther.* **20**, 501–509 (2014).

66. Wang, G., Li, X. & Wang, Z. APD3: the antimicrobial peptide database as a tool for research and education. *Nucleic Acids Res.* **44**, D1087–D1093 (2016).

67. Eisenstein, B. I., Oleson, F. B. & Baltz, R. H. Daptomycin: From the Mountain to the Clinic,with Essential Help from Francis Tally, MD. doi:10.1086/647938.

68. Lamp, K. C., Friedrich, L. V., Mendez-Vigo, L. & Russo, R. Clinical Experience with Daptomycin for the Treatment of Patients with Osteomyelitis. *Am. J. Med.* **120**, S13–S20 (2007).

69. Piper, K. E., Steckelberg, J. M., Patel, R. & Patel, R. In vitro activity of daptomycin against clinical isolates of Gram-positive bacteria. *J. Infect. Chemother.* **11**, 207–209 (2005).

70. Micklefield, J. Daptomycin Structure and Mechanism of Action Revealed. *Chem. Biol.* **11**, 887–888 (2004).

71. Lee, M.-T. *et al.* Molecular State of the Membrane-Active Antibiotic Daptomycin. *Biophys. J.* **113**, 82–90 (2017).

72. Sugawara, E. & Nikaido, H. Properties of AdeABC and AdeIJK efflux systems of Acinetobacter baumannii compared with those of the AcrAB-TolC system of Escherichia

coli. *Antimicrob. Agents Chemother.* **58**, 7250–7 (2014).

73. Sing, K. S. W. Reporting physisorption data for gas/solid systems with special reference to the determination of surface area and porosity (Recommendations 1984). *Pure Appl. Chem.* **57**, 603–619 (1985).

74. John, A.-K. *et al.* Efficacy of Daptomycin in Implant-Associated Infection Due to Methicillin-Resistant *Staphylococcus aureus* : Importance of Combination with Rifampin. *Antimicrob. Agents Chemother.* **53**, 2719–2724 (2009).